System Characterization Report on PRecursore IperSpettrale della Missione Applicativa (PRISMA)

Chapter K of
System Characterization of Earth Observation Sensors

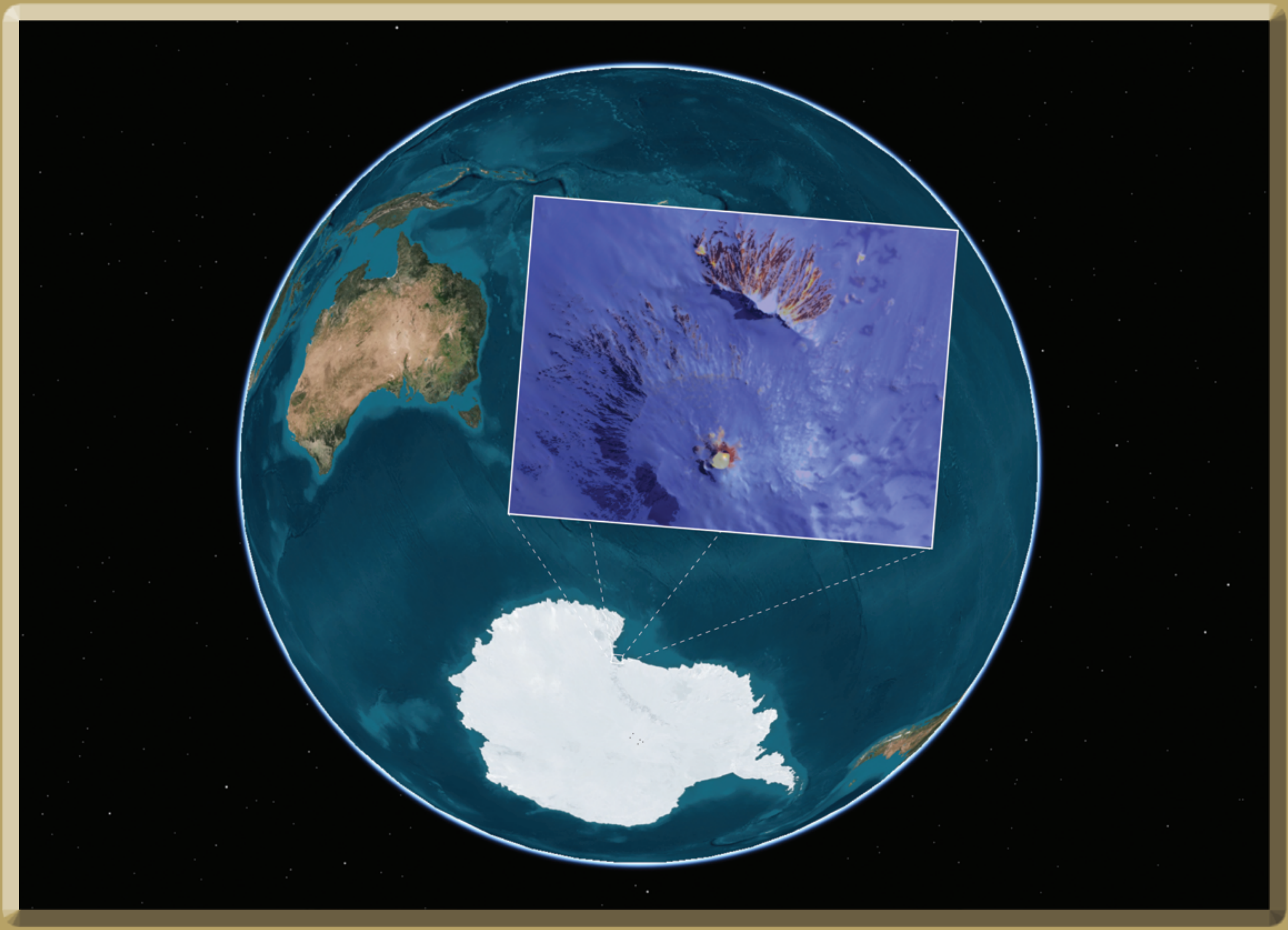

Open-File Report 2021–1030–K

U.S. Department of the Interior
U.S. Geological Survey

Cover: The satellite image, acquired by PRecursore IperSpettrale della Missione Applicativa (PRISMA) on December 8, 2021, shows the Erebus volcano on Ross Island (Antarctica), in a pansharpening of shortwave infrared processing. Erebus is the most southern active volcano on Earth. Reddish colors indicate points at higher reflection (or emission) in bands of the electromagnetic spectrum that are closer to the thermal infrared band. On the lower (southern) part of the image, the hot volcanic caldera is shown. Also shown are the different shortwave infrared traces of the flanks of the volcano exposed to direct sunlight (toward the north and northeast) compared to the flanks exposed to shadow (toward the south and southwest). Data and information generated by Gabriele Impresario, Agenzia Spaziale Italiana, under an ASI License to Use. Original PRISMA Product, Image of Earth from Analytical Graphics, Inc., Systems Tool Kit.

System Characterization Report on PRecursore IperSpettrale della Missione Applicativa (PRISMA)

By Minsu Kim,[1] Seonkyung Park,[1] Cody Anderson,[2] and Gregory L. Stensaas[2]

Chapter K of

System Characterization of Earth Observation Sensors

Compiled by Shankar N. Ramaseri Chandra[1]

[1]KBR, Inc., under contract to the U.S. Geological Survey.

[2]U.S. Geological Survey.

Open-File Report 2021–1030–K

U.S. Department of the Interior
U.S. Geological Survey

U.S. Geological Survey, Reston, Virginia: 2022

For more information on the USGS—the Federal source for science about the Earth, its natural and living resources, natural hazards, and the environment—visit https://www.usgs.gov or call 1–888–ASK–USGS.

For an overview of USGS information products, including maps, imagery, and publications, visit https://store.usgs.gov/.

Suggested citation:
Kim, M., Park, S., Anderson, C., and Stensaas, G.L., 2022, System characterization report on PRecursore IperSpettrale della Missione Applicativa (PRISMA), chap. K *of* Ramaseri Chandra, S.N., comp., System characterization of Earth observation sensors: U.S. Geological Survey Open-File Report 2021–1030, 28 p., https://doi.org/10.3133/ofr20211030K.

ISSN 2331-1258 (online)

Contents

Figures

Tables

Conversion Factors

International System of Units to U.S. customary units

Multiply	By	To obtain
	Length	
nanometer (nm)	3.9370×10^{-8}	inch (in.)
micrometer (µm)	3.9370×10^{-5}	inch (in.)
meter (m)	3.281	foot (ft)
meter (m)	1.094	yard (yd)
kilometer (km)	0.6214	mile (mi)

Abbreviations

CE90	circular error at 90 percent
ECCOE	Earth Resources Observation and Science Cal/Val Center of Excellence
GCP	ground control point
JACIE	Joint Agency Commercial Imagery Evaluation
OLI	Operational Land Imager
PRISMA	PRecursore IperSpettrale della Missione Applicativa
USGS	U.S. Geological Survey

System Characterization Report on PRecursore IperSpettrale della Missione Applicativa (PRISMA)

By Minsu Kim,[1] Seonkyung Park,[1] Cody Anderson,[2] and Gregory L. Stensaas[2]

Executive Summary

This report addresses system characterization of the Italian Space Agency's PRecursore IperSpettrale della Missione Applicativa (PRISMA) and is part of a series of system characterization reports produced and delivered by the U.S. Geological Survey Earth Resources Observation and Science Cal/Val Center of Excellence. These reports present and detail the methodology and procedures for characterization; present technical and operational information about the specific sensing system being evaluated; and provide a summary of test measurements, data retention practices, data analysis results, and conclusions.

The Earth Resources Observation and Science Cal/Val Center of Excellence system characterization team completed data analyses to characterize the geometric (band to band and image to image), radiometric, and spatial performances. Results of these analyses indicate that PRISMA has a band-to-band geometric performance in the range of −0.046 to 0.040 pixel; an image-to-image geometric performance (relative to the Landsat 8 Operational Land Imager) in the range of −60.791 meters (m; −2.03 pixels) to 299.541 m (9.98 pixels); a radiometric performance in the range of −0.037 to −0.001 in offset and 1.026 to 1.274 in slope; and a spatial performance with a relative edge response in the range of 0.56 to 0.63, full width at half maximum in the range of 1.84 to 1.97 pixels, and a modulation transfer function at a Nyquist frequency in the range of 0.054 to 0.096. Regarding fairly large geometric accuracy, the following explanation is provided to help the reader. The geometric accuracy required for PRISMA is a 200-m circular error at 90 percent (CE90) without ground control points (GCPs), a 15-m CE90 using GCPs is documented in the PRISMA mission overview (Agenzia Spaziale Italiana, 2021). The PRISMA images used for the current system characterization were georeferenced without using any GCPs; thus, the 200-m geometric accuracy requirement is applied. Beginning in 2022, a worldwide GCP database will be used in the PRISMA product processing chain, which will improve georeferencing accuracy to meet the 15-m CE90 requirement.

[1]KBR, Inc., under contract to the U.S. Geological Survey.

[2]U.S. Geological Survey.

Reference Cited

Agenzia Spaziale Italiana, 2021, PRISMA: Agenzia Spaziale Italiana web page, accessed March 2021 at https://www.asi.it/en/earth-science/prisma/.

Introduction

The Italian Space Agency's PRecursore IperSpettrale della Missione Applicativa (PRISMA) is a hyperspectral electro-optical sensor that analyzes the chemical-physical composition of the objects present in the scene. The PRISMA sensor offers the scientific community and users many applications in the fields of environmental monitoring, resource management, crop classification, pollution control, and other areas. The mission objective is to provide a global observation capability with the specific areas of interest over Europe and the Mediterranean region. Characterization of the PRISMA requires additional spectral resampling for the system characterization compared to the conventional multi spectral sensor because it is a hyperspectral imager.

The data analysis results provided in this report have been derived from approved Joint Agency Commercial Imagery Evaluation (JACIE) processes and procedures. JACIE was formed to leverage resources from several Federal agencies for the characterization of remote sensing data and to share those results across the remote sensing community. More information about JACIE is available at https://www.usgs.gov/calval/jacie?qt-science_support_page_related_con=3#qt-science_support_page_related_con.

Purpose and Scope

The purpose of this report is to describe the specific sensor or sensing system, test its performance in three categories, complete related data analyses to quantify these performances, and report the results in a standardized document. In this chapter, the PRISMA sensor is described. The performance testing of the system is limited to geometric, radiometric, and spatial analyses. The scope of the geometric assessment is limited to testing band-to-band alignments and image-to-image relative georeferencing error is tested in reference to the Landsat 8 Operational Land Imager (OLI).

The U.S. Geological Survey (USGS) Earth Resources Observation and Science Cal/Val Center of Excellence (ECCOE) project, and the associated system characterization process used for this assessment, follows the USGS Fundamental Science Practices, which include maintaining data, information, and documentation needed to reproduce and validate the scientific analysis documented in this report. Additional information and guidance about Fundamental Science Practices and related resource information of interest to the public are available at https://www.usgs.gov/office-of-science-quality-and-integrity/fundamental-science-practices. For additional information related to the report, please contact ECCOE at eccoe@usgs.gov.

System Description

This section describes the satellite and operational details and provides information about the PRISMA sensor. The satellite and operational details for the PRISMA sensor are listed in table 1. The imaging sensor details for PRISMA are listed in table 2.

Table 1. Satellite and operational details for the Italian Space Agency's PRecursore IperSpettrale della Missione Applicativa sensor.

[PRISMA, PRecursore IperSpettrale della Missione Applicativa; km, kilometer; °, degree; ±, plus or minus; m, meter]

Product information	PRISMA data
Satellite and operational information	
Sensor name	PRISMA
Sensor type	Hyperspectral
Mission type	Global land-monitoring mission
Launch date	March 22, 2019
Expected lifetime	5 years
Operational details	
Operating orbit	Sun-synchronous orbit
Orbital altitude range	620 km
Sensor angle altitude	97.85° inclination
Imaging time	10:35 a.m. (local time of equator crossing on descending node)
Geographic coverage	30 km (field of view, 2.45°)
Temporal resolution	29 days
Temporal coverage	2019 to present (2021)
Imaging angles	±30°
Ground sample distance	30 m
Product abstract	http://prisma-i.it/index.php/en/

Table 2. Imaging sensor details for the Italian Space Agency's PRecursore IperSpettrale della Missione Applicativa.

[PRISMA, PRecursore IperSpettrale della Missione Applicativa; µm, micrometer; GSD, ground sample distance; m, meter; FWHM, full width at half maximum; nm, nanometer; VNIR, visible near infrared; SW, shortwave infrared]

Spectral band details	PRISMA				
	Lower bound (µm)	Upper bound (µm)	Radiometric resolution (bits)	GSD (m)	FWHM (nm)
VNIR (66 channels)	0.400	1.010	12	30.0	12
SW (171 channels)	0.920	2.505	12	30.0	12

Procedures

ECCOE has established standard processes to identify Earth observing systems of interest and to assess the geometric, radiometric, and spatial qualities of data products from these systems.

The assessment steps are as follows:

- system identification and investigation to learn the general specifications of the satellite and its sensor(s);
- data receipt and initial inspection to understand the characteristics and any overt flaws in the data product so that it may be further analyzed;
- geometry characterization, including band-to-band geometric error measuring the relative alignment of spectral bands and image-to-image relative georeferencing error measuring how well the georeferenced pixels of the comparison sensor image are aligned to the reference sensor image;
- radiometry characterization, including assessing how well the data product correlates with a known reference and, when possible, assessing the signal-to-noise ratio; and
- spatial characterization, assessing the two-dimensional fidelity of the image pixels to their projected ground sample distance.

The specific procedures required to handle hyperspectral data are as follows:

- correction of the defective pixel that causes a dark striping,
- spectral resampling of hyperspectral data to match the spectral response function of the Landsat 8 OLI, and
- computation of solar irradiance by resampling high resolution extraterrestrial solar irradiance based on the spectral response function of the Landsat 8 OLI.

Data analysis and test results are maintained at the USGS Earth Resources Observation and Science Center by the ECCOE project.

Measurements

The observed USGS measurements are listed in table 3. Details about the methodologies used are outlined in the “Analysis” section.

Table 3. U.S. Geological Survey measurement results.

[VNIR, visible near infrared; nm, nanometer; STDDEV, standard deviation; RMSE, root mean square error; SW, shortwave infrared; OLI, Landsat 8 Operational Land Imager; m, meter; R^2, coefficient of determination; %, percent; PRISMA, PRecursore IperSpettrale della Missione Applicativa; NIR, near infrared; RER, relative edge response; FWHM, full width at half maximum; MTF, modulation transfer function; USGS, U.S. Geological Survey]

Description of product	System characterization results
Geometric performance (easting, northing)	
Band to band	VNIR (641.3-nm reference, band 31): Mean: −0.042 to 0.015 pixel, −0.028 to 0.031 pixel STDDEV: 0.041 to 0.095 pixel, 0.040 to 0.078 pixel RMSE: 0.042 to 0.100 pixel, 0.041 to 0.083 pixel SW (1,793.7-nm reference, band 85): Mean: −0.046 to 0.040 pixel, −0.051 to 0.052 pixel STDDEV: 0.035 to 0.131 pixel, 0.040 to 0.102 pixel RMSE: 0.035 to 0.138 pixel, 0.042 to 0.107 pixel
Image to image (against OLI)	Easting mean: 75.339 to 299.541 m (2.51 to 9.98 pixels) Easting RMSE: 79.564 to 315.585 m (2.65 to 10.52 pixels) Northing mean: −60.791 to 240.069 m (−2.03 to 8.00 pixels) Northing RMSE: 61.693 to 241.866 m (2.06 to 8.06 pixels)
Radiometric performance (offset, slope, R^2, uncertainty [%])	
Radiometric evaluation (linear regression—PRISMA versus OLI reflectance)	Band 1—coastal blue: −0.027 to −0.012, 1.047 to 1.159, 0.697 to 0.801, 2.46 to 5.91 Band 2—blue: −0.015 to −0.006, 1.026 to 1.098, 0.710 to 0.817, 3.70 to 8.23 Band 3—green: −0.016 to −0.003, 1.047 to 1.125, 0.713 to 0.822, 5.28 to 9.88 Band 4—red: −0.011 to −0.003, 1.042 to 1.129, 0.725 to 0.837, 11.54 to 18.18 Band 5—NIR: −0.037 to −0.002, 1.057 to 1.085, 0.754 to 0.798, 8.08 to 11.44 Band 6—SW1: −0.037 to −0.001, 1.063 to 1.147, 0.744 to 0.813, 10.39 to 13.92 Band 7—SW2: −0.018 to −0.005, 1.200 to 1.274, 0.738 to 0.826, 17.43 to 20.43
Spatial performance	
Spatial performance measurement	RER: 0.56 to 0.63 FWHM: 1.84 to 1.97 pixels MTF at Nyquist: 0.054 to 0.096
Known artifacts and quality issues	
USGS noted artifacts/quality issues	Because of the large pixel, the calibration site is not large enough; thus, spatial analysis results are associated with higher uncertainty.

Analysis

This section of the report describes the geometric, radiometric, and spatial performance of the PRISMA sensor.

Geometric Performance

The geometric performance for PRISMA is characterized in terms of the band-to-band alignment and image-to-image relative geometric accuracy.

Band-to-Band Performance

Band-to-band analysis reveals the geometric error between different bands using cross-correlation matrix. For this analysis, each band of the PRISMA imagery was registered against one reference band. For the visible near-infrared bands, a band centered at 641 nanometers (band 31) was used as a reference. For the shortwave infrared bands, a band centered at 1,793.7 nanometers was used. The relative differences are less than 5 percent of a pixel, which indicates a high quality of band-to-band performance. The scene identifier used as an example image to compute the band-to-band error is PRS_L1_STD_OFFL_20200412034634_20200412034638_0001, which is shown in figure 1.

The grid system and error vectors for band 30 are shown in figure 1 as an example. The red arrows show the relative error vector for each yellow grid, where the x and y vector components represent the easting and northing errors. Several grids with missing arrows represent the outliers. The mean and root mean square error values are computed from the grids for band 30 and represent the dots for band 30 in figures 2 and 3.

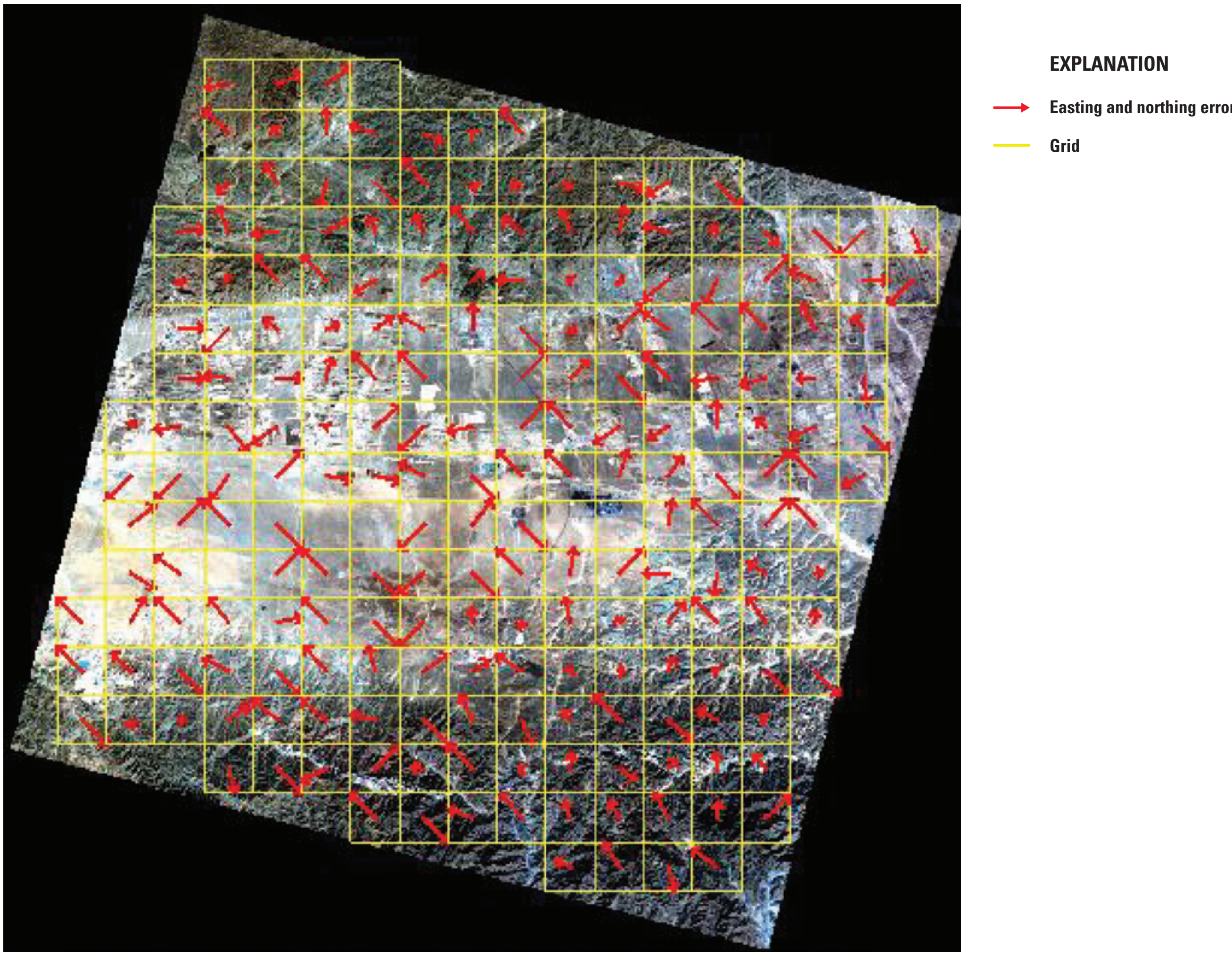

Figure 1. Band-to-band geometric error of band 30 using band 31 as a reference.

Band-to-band full shortwave infrared spectral geometric error estimation was completed using band 85 as a reference. The results are shown in figure 4 for the easting error and in figure 5 for the northing error. Compared to visible near-infrared bands, there are two noisy spectral regions centered around 1.4 micrometers and 1.9 micrometers, which is the strong absorption band from atmospheric water vapor.

Image-to-Image Performance

Image-to-image analysis measures relative georeferencing error between the comparison sensor image and reference sensor image using cross-correlation matrix. For this analysis, a spectrally resampled PRISMA image was used. The resampling was based on the spectral response of the Landsat 8 OLI. Three scene pairs between PRISMA and the Landsat 8 OLI were used for image-to-image analysis. A normalized cross-correlation matrix was computed, and its local maxima were determined to estimate the mean error and root mean square error. The results, which are represented in pixels at a 30-meter ground sample distance, are listed in table 4. For each of the three PRISMA images, geometric error maps showing the directional shift and relative magnitude of the shift, when compared with the Landsat 8 OLI, are provided in figures 6 through 11. Regarding fairly large geometric accuracy, the following explanation is provided to help the reader. The geometric accuracy required for PRISMA is a 200-m circular error at 90 percent (CE90) without ground control points (GCPs), a 15-m CE90 using GCPs is documented in the PRISMA mission overview (Agenzia Spaziale Italiana, 2021). The PRISMA images used for the current system characterization were georeferenced without using any GCPs; thus, the 200-m geometric accuracy requirement is applied. Beginning in 2022, a worldwide GCP database will be used in the PRISMA product processing chain, which will improve georeferencing accuracy to meet the 15-m CE90 requirement.

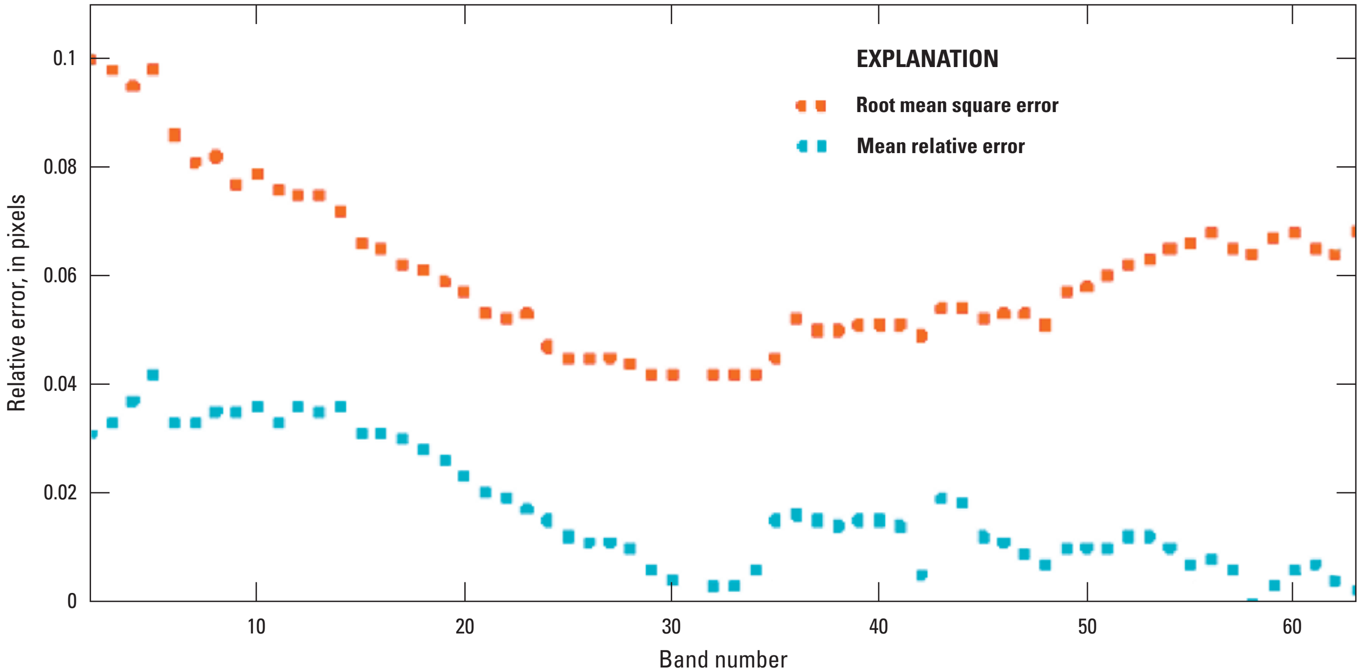

Figure 2. Visible near-infrared band-to-band easting geometric errors using band 31 as a reference.

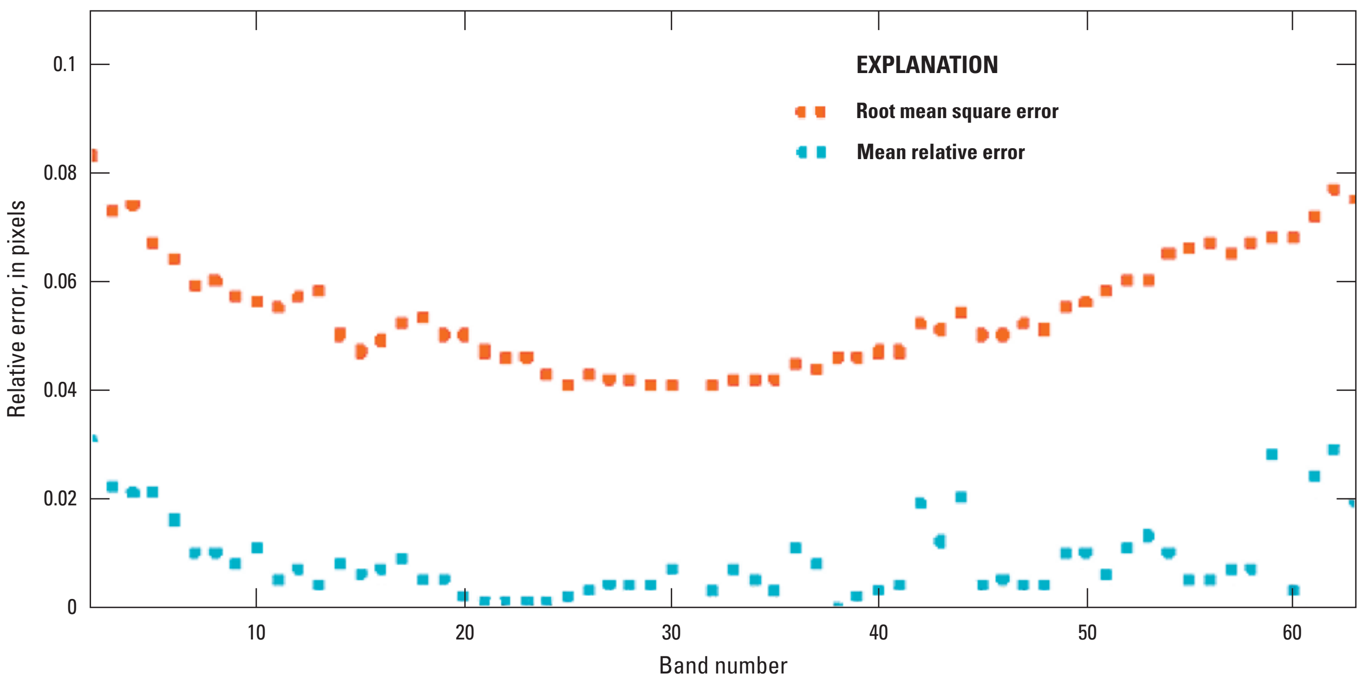

Figure 3. Visible near-infrared band-to-band northing geometric errors using band 31 as a reference.

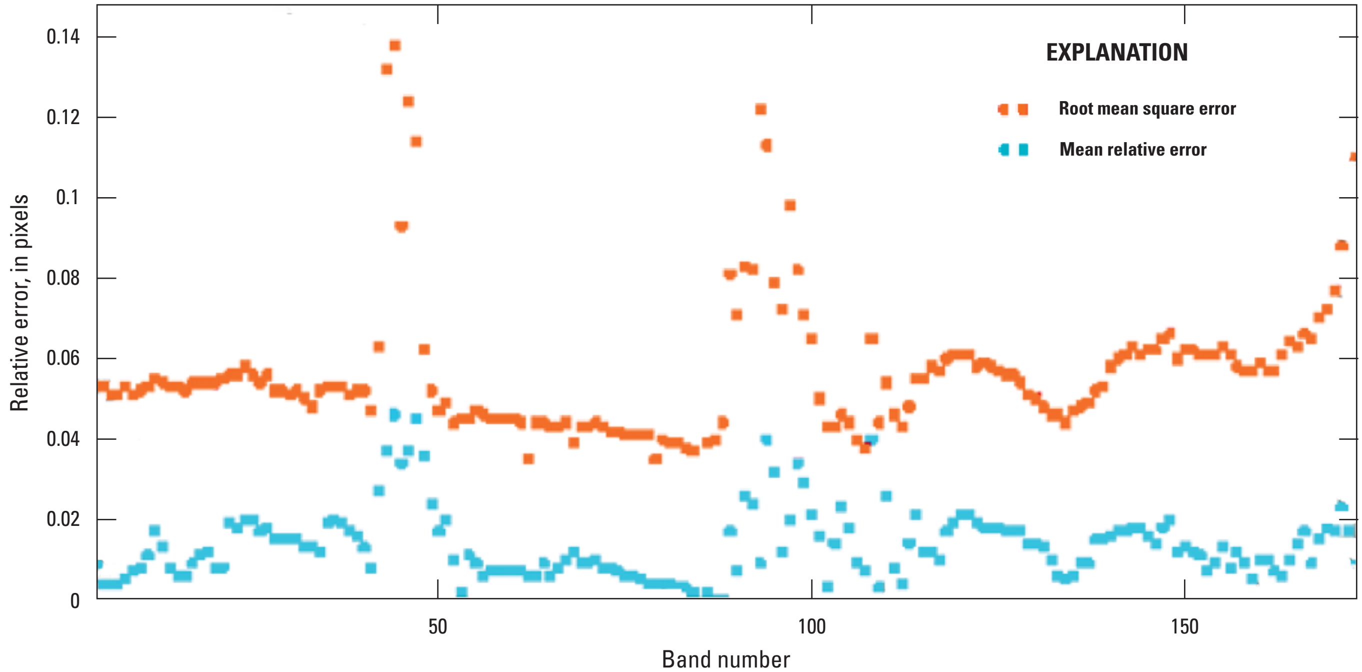

Figure 4. Shortwave-infrared band-to-band easting geometric error using band 85 as a reference.

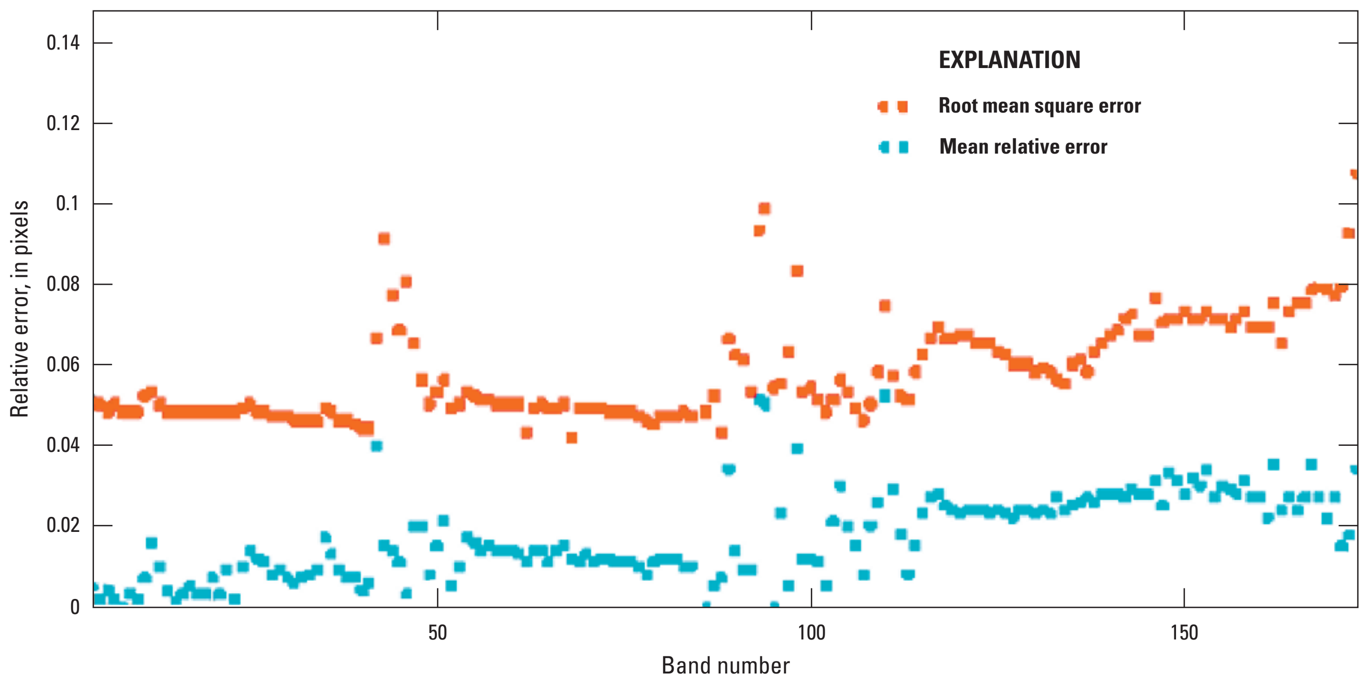

Figure 5. Shortwave-infrared band-to-band northing geometric error using band 85 as a reference.

Table 4. Geometric error of the Italian Space Agency's PRecursore IperSpettrale della Missione Applicativa relative to Landsat 8 Operational Land Imager imagery.

[ID, identifier; RMSE, root mean square error; m, meter]

Scene ID	Mean error (easting)	Mean error (northing)	RMSE (easting)	RMSE (northing)
PRS_L1_STD_OFFL_20200426091752_20200426091756_0001 versus LC08_L1TP_182031_20200426_20200822_02_T1 (Kyprinos, Greece)	75.339 m (2.51 pixels)	115.181 m (3.84 pixels)	79.564 m (2.65 pixels)	116.715 m (3.89 pixels)
PRS_L1_STD_OFFL_20200509094105_20200509094109_0001 versus LC08_L1TP_186031_20200508_20200820_02_T1 (Shkodër, Albania)	299.541 m (9.98 pixels)	240.069 m (8.00 pixels)	315.585 m (10.52 pixels)	241.866 m (8.06 pixels)
PRS_L1_STD_OFFL_20200729111312_20200729111317_0001 versus LC08_L1TP_200028_20200729_20200908_02_T1 (La Roche-sur-Yon, France)	115.094 m (3.84 pixels)	−60.791 m (−2.03 pixels)	116.164 m (3.87 pixels)	61.693 m (2.06 pixels)

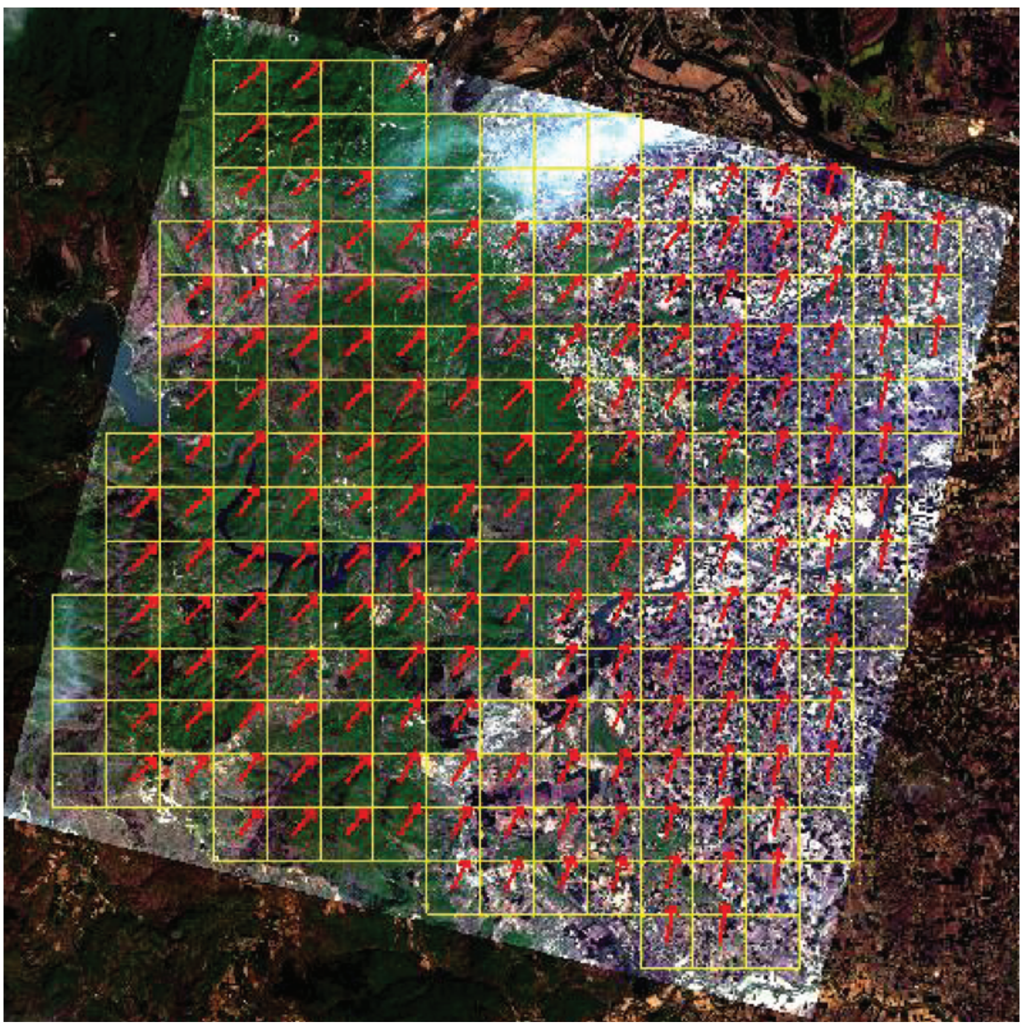

Figure 6. Image-to-image geometric error map using image pair (Kyprinos, Greece).

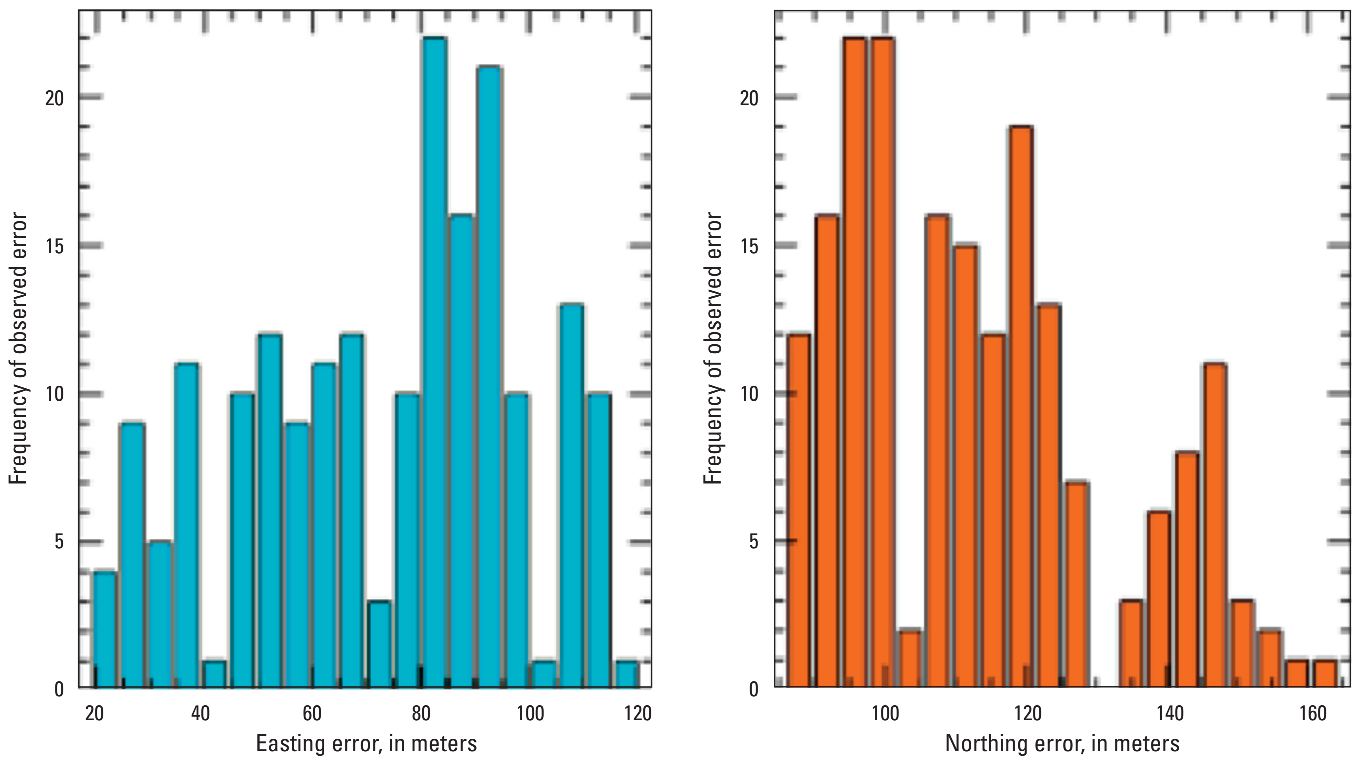

Figure 7. Histogram of image-to-image geometric error using image pair (Kyprinos, Greece).

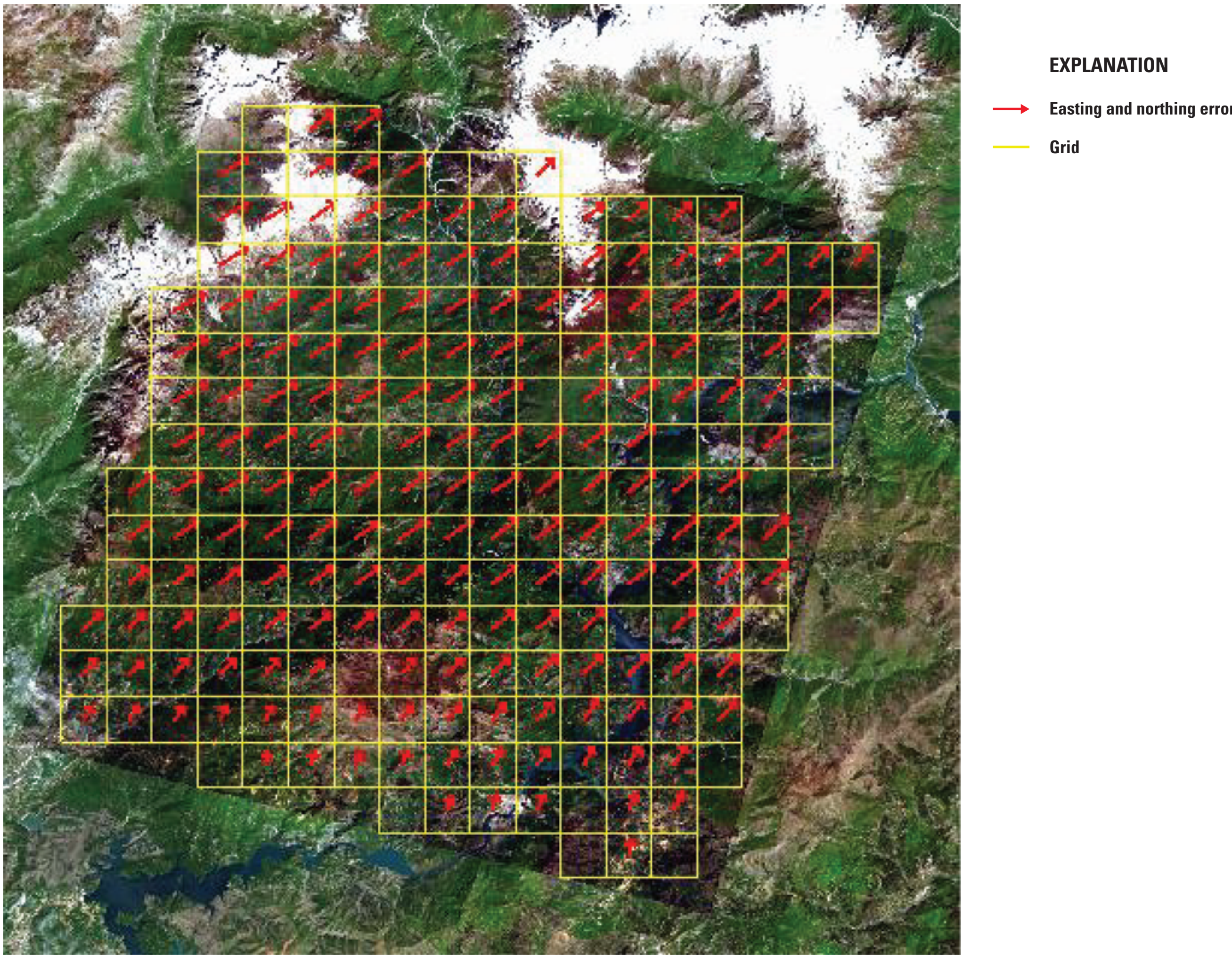

Figure 8. Image-to-image geometric error map using image pair (Shkodër, Albania).

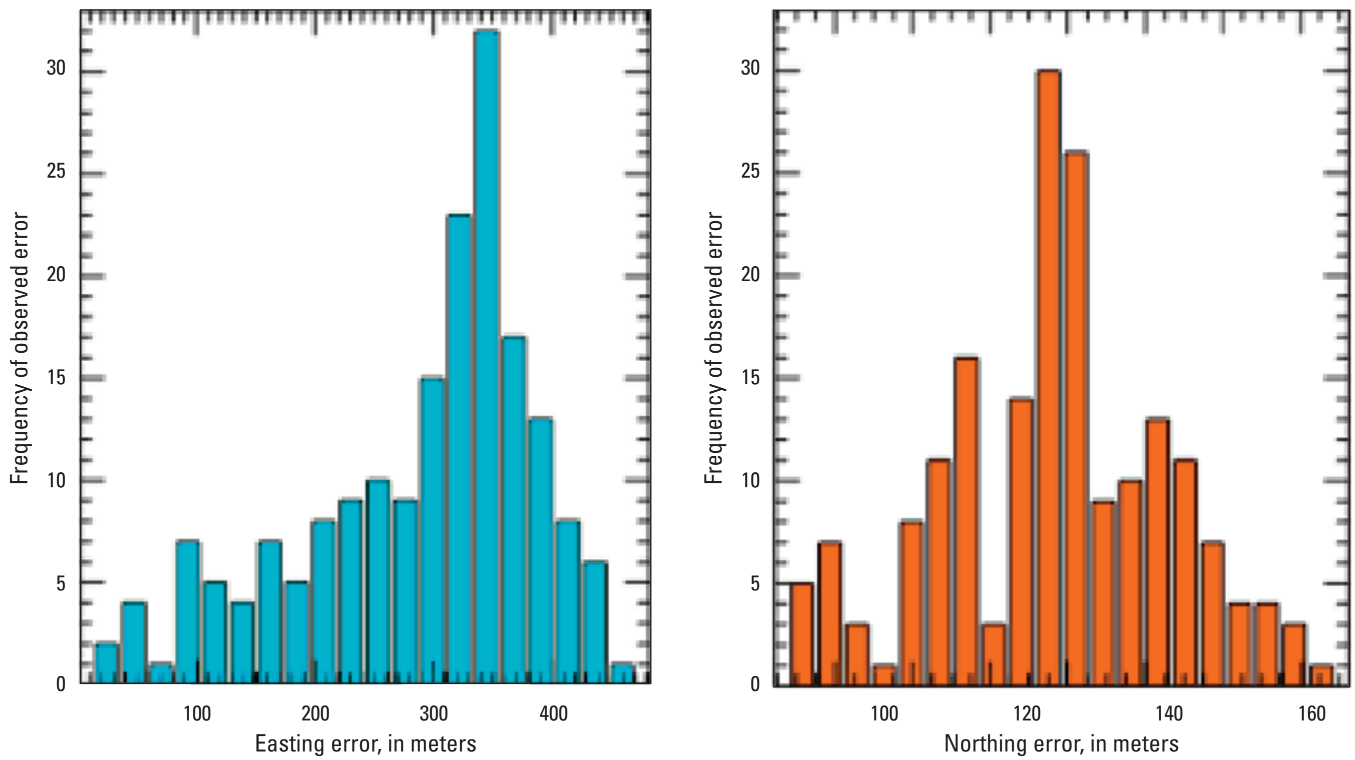

Figure 9. Histogram of image-to-image geometric error using image pair (Shkodër, Albania).

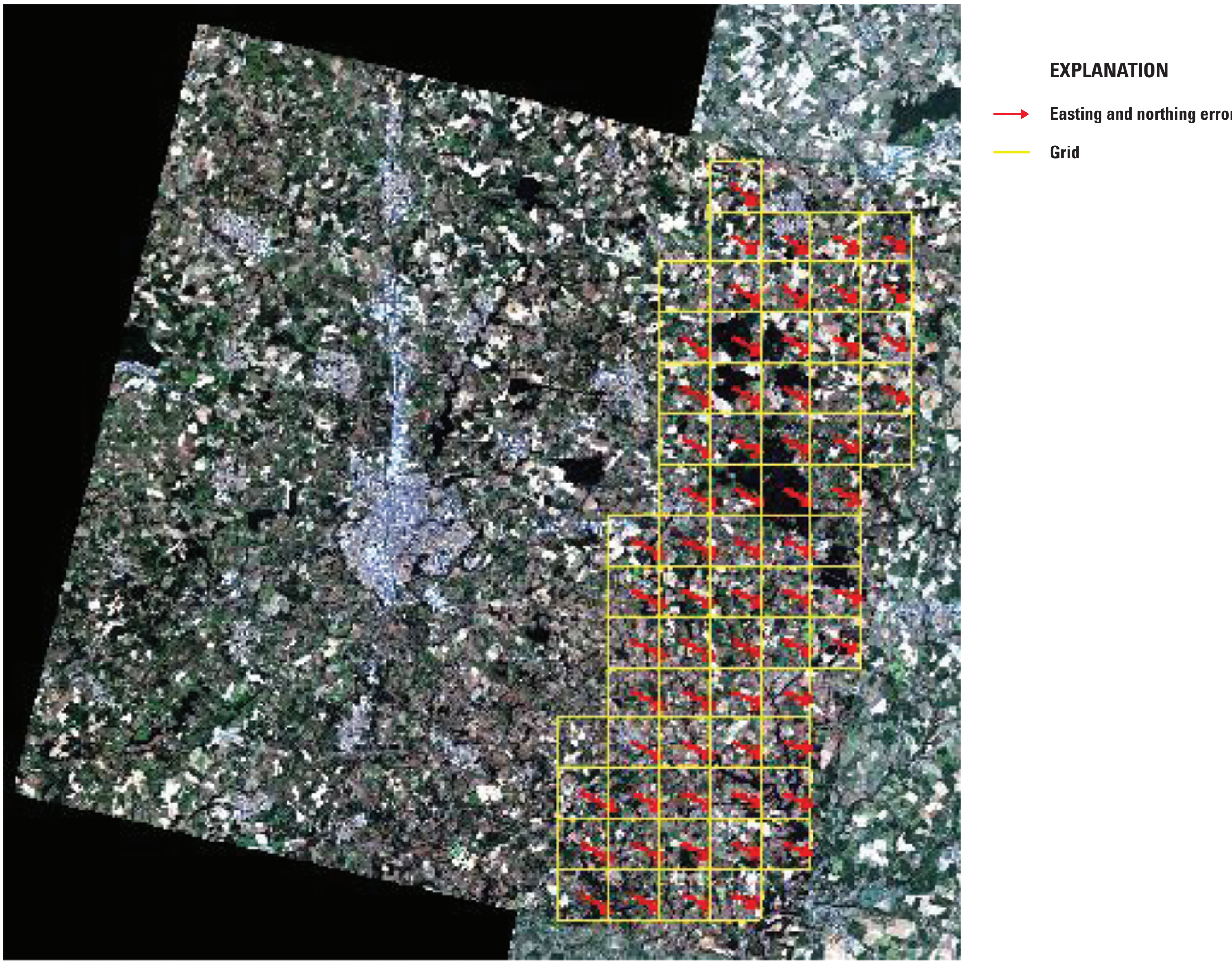

Figure 10. Image-to-image geometric error map using image pair (La Roche-sur-Yon, France).

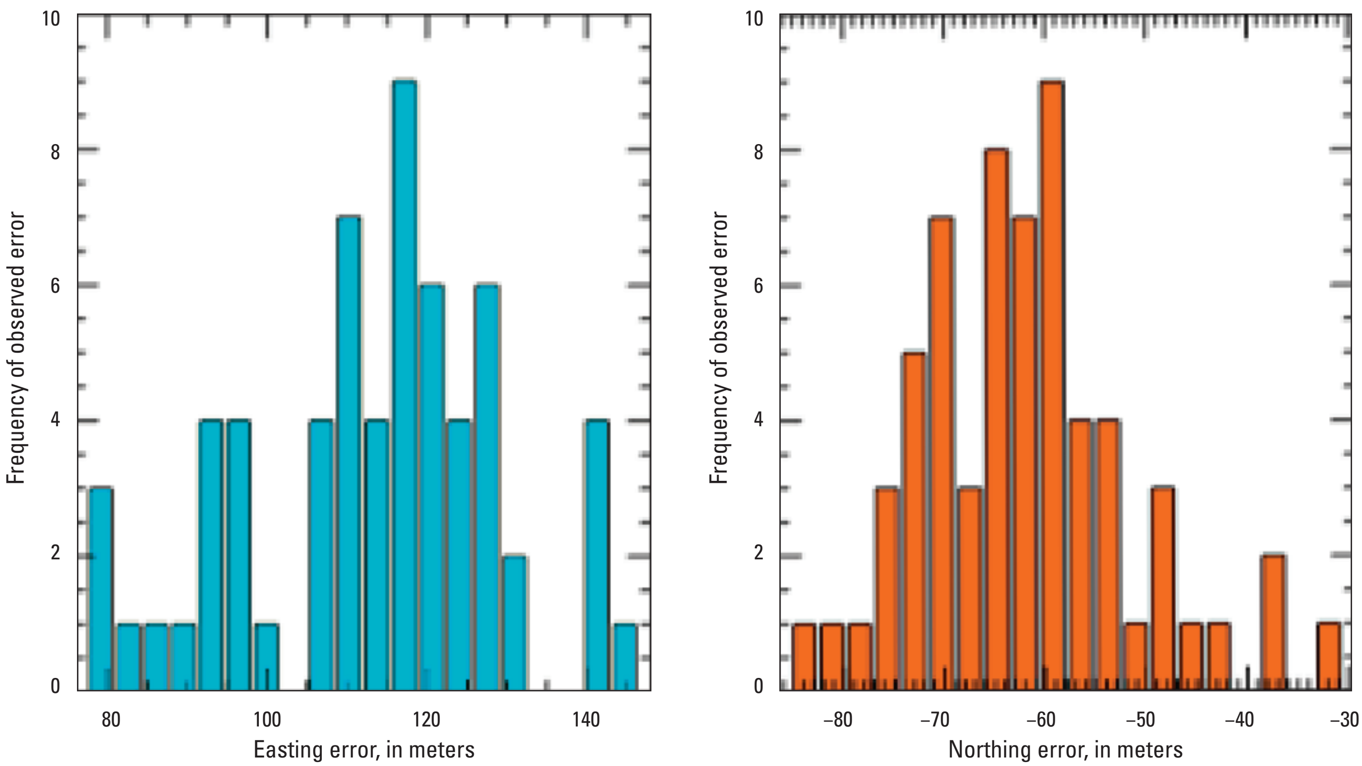

Figure 11. Histogram of image-to-image geometric error using image pair (La Roche-sur-Yon, France).

Radiometric Performance

For this analysis, cloud-free regions of interest were selected within three near-coincident PRISMA and Landsat 8 OLI scene pairs. Top of Atmosphere reflectance comparison results are listed in table 5. Once the relative georeferencing error between Landsat 8 OLI and PRISMA has been corrected, Top of Atmosphere reflectance values from the two sensors are extracted. The scatterplots, figures 12 through 14, are drawn in a way that the x-axis is the reference sensor and the y-axis is the comparison sensor. The linear regression, thus, represents Top of Atmosphere reflectance relative to that of the reference sensor. Ideally, the slope should be near unity and the offset should be near zero. For instance, if the slope is greater than unity, that means the comparison sensor has a tendency to overestimate Top of Atmosphere reflectance compared to the reference sensor. A band-by-band graphical comparison over scene 1 is shown in figure 12, a comparison over scene 2 is shown in figure 13, and a comparison over scene 3 is shown in figure 14.

Table 5. Top of Atmosphere reflectance comparison for the Italian Space Agency's PRecursore IperSpettrale della Missione Applicativa with Landsat 8 Operational Land Imager.

[ID, identifier; B, band; CB, coastal blue; NIR, near infrared; SW, shortwave infrared; %, percent; R^2, coefficient of determination]

Scene ID	Statistics	B1 (CB)	B2 (blue)	B3 (green)	B4 (red)	B5 (NIR)	B6 (SW1)	B7 (SW2)
PRS_L1_STD_OFFL_20200426091752_20200426091756_0001 versus LC08_L1TP_182031_20200426_20200822_02_T1 (Kyprinos, Greece)	Uncertainty (%)	2.46	3.70	5.28	11.54	9.18	10.39	17.43
	R^2	0.733	0.767	0.756	0.781	0.798	0.787	0.790
	Regression offset	−0.027	−0.015	−0.016	−0.011	−0.024	−0.024	−0.016
	Regression slope	1.159	1.098	1.125	1.129	1.085	1.147	1.274
PRS_L1_STD_OFFL_20200509094105_20200509094109_0001 versus LC08_L1TP_186031_20200508_20200820_02_T1 (Shkodër, Albania)	Uncertainty (%)	5.91	8.23	9.88	18.18	11.44	13.92	20.43
	R^2	0.697	0.710	0.713	0.725	0.754	0.744	0.738
	Regression offset	−0.012	−0.006	−0.003	−0.003	−0.002	−0.001	−0.005
	Regression slope	1.112	1.075	1.064	1.096	1.057	1.063	1.214
PRS_L1_STD_OFFL_20200729111312_20200729111317_0001 versus LC08_L1TP_200028_20200729_20200908_02_T1 (La Roche-sur-Yon, France)	Uncertainty (%)	4.44	6.61	9.56	16.3	8.08	13.11	19.35
	R^2	0.801	0.817	0.822	0.837	0.785	0.813	0.826
	Regression offset	−0.019	−0.014	−0.013	−0.010	−0.037	−0.037	−0.018
	Regression slope	1.047	1.026	1.047	1.042	1.064	1.125	1.200

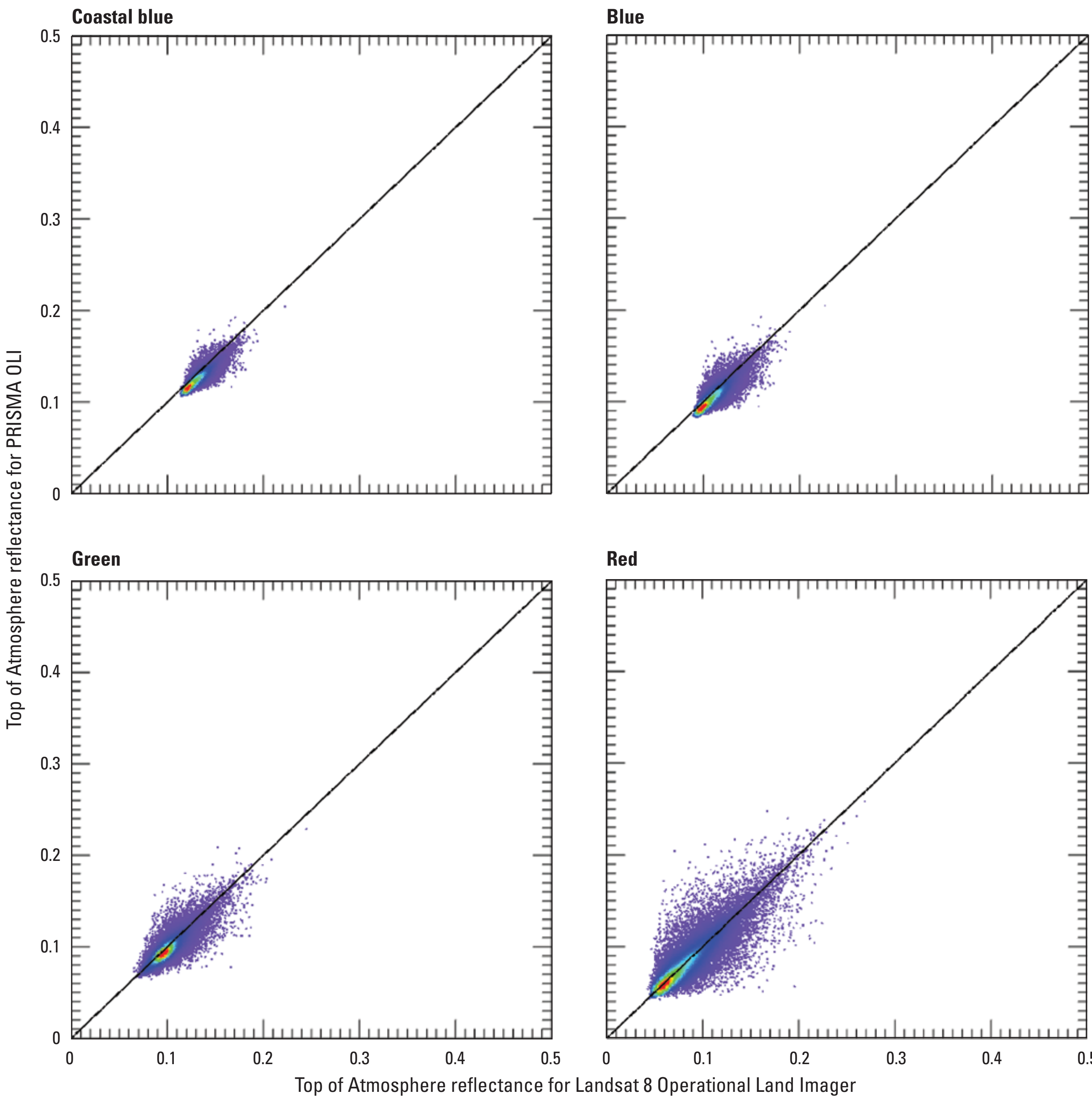

Figure 12. Top of Atmosphere reflectance comparison using image pair (Kyprinos, Greece). [PRISMA OLI, PRecursore IperSpettrale della Missione Applicativa mimicking Operational Land Imager bands]

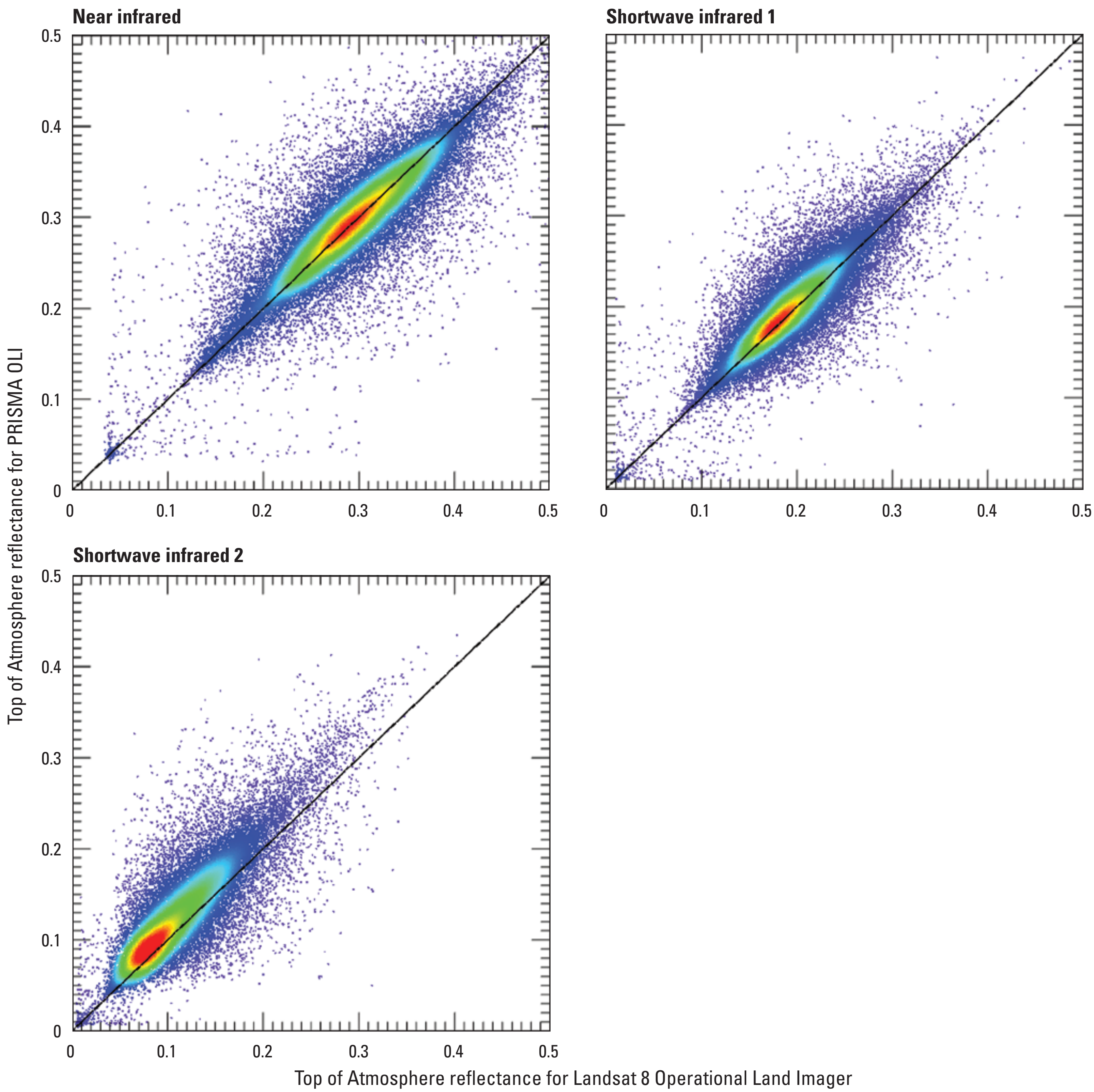

Figure 12. Top of Atmosphere reflectance comparison using image pair (Kyprinos, Greece). [PRISMA OLI, PRecursore IperSpettrale della Missione Applicativa mimicking Operational Land Imager bands]—Continued

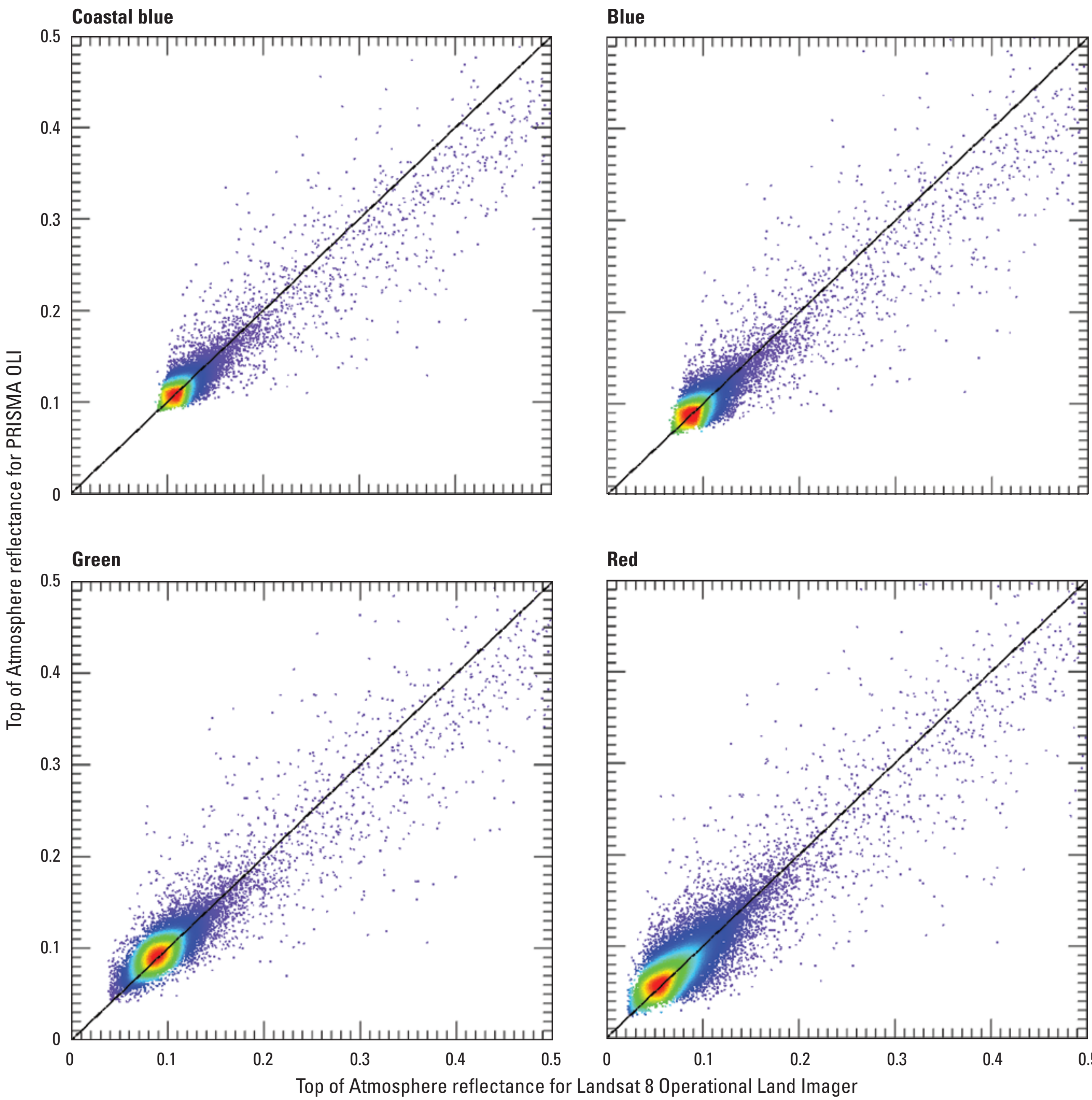

Figure 13. Top of Atmosphere reflectance comparison using image pair (Shkodër, Albania). [PRISMA OLI, PRecursore IperSpettrale della Missione Applicativa mimicking Operational Land Imager bands]

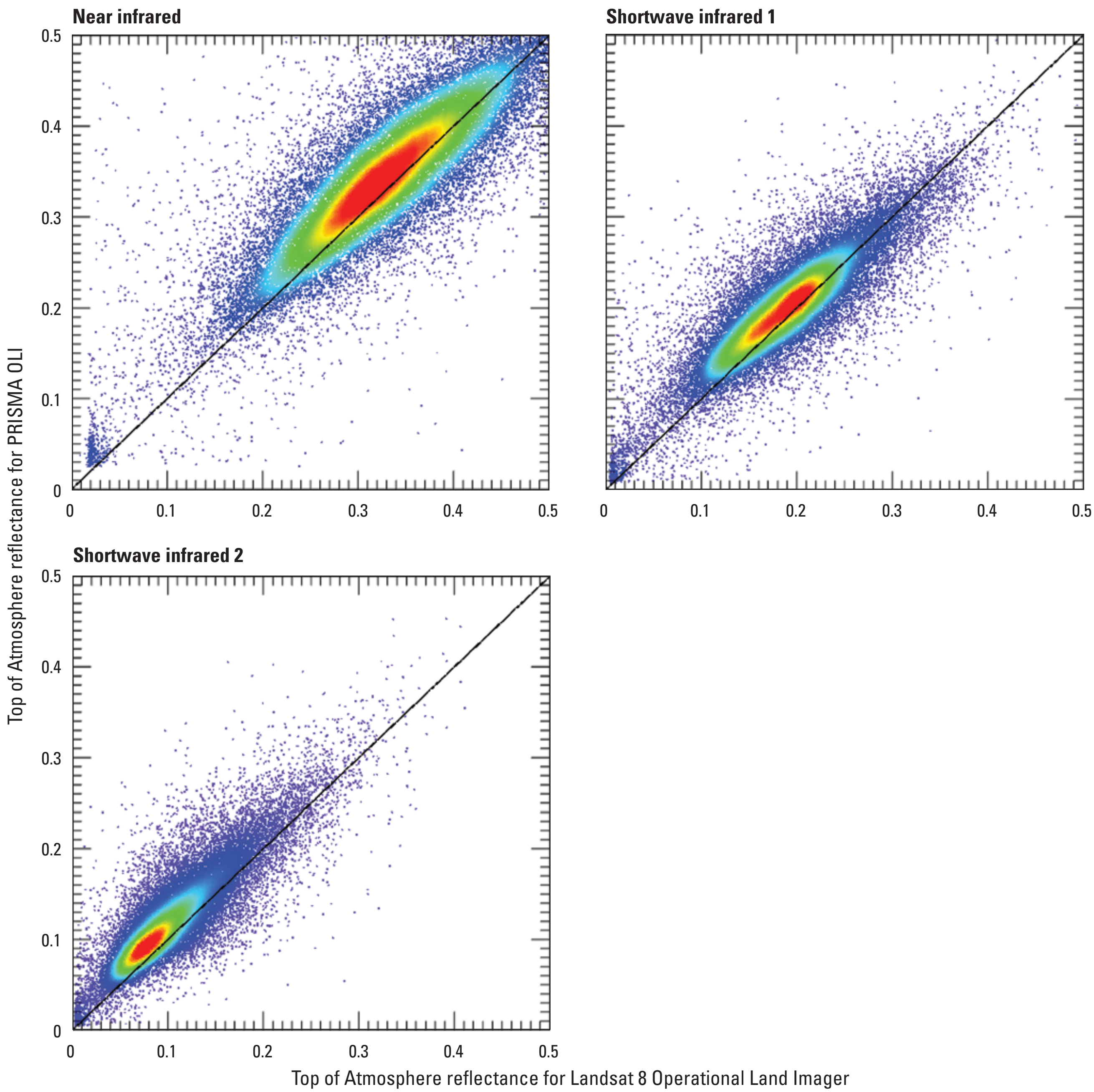

Figure 13. Top of Atmosphere reflectance comparison using image pair (Shkodër, Albania). [PRISMA OLI, PRecursore IperSpettrale della Missione Applicativa mimicking Operational Land Imager bands]—Continued

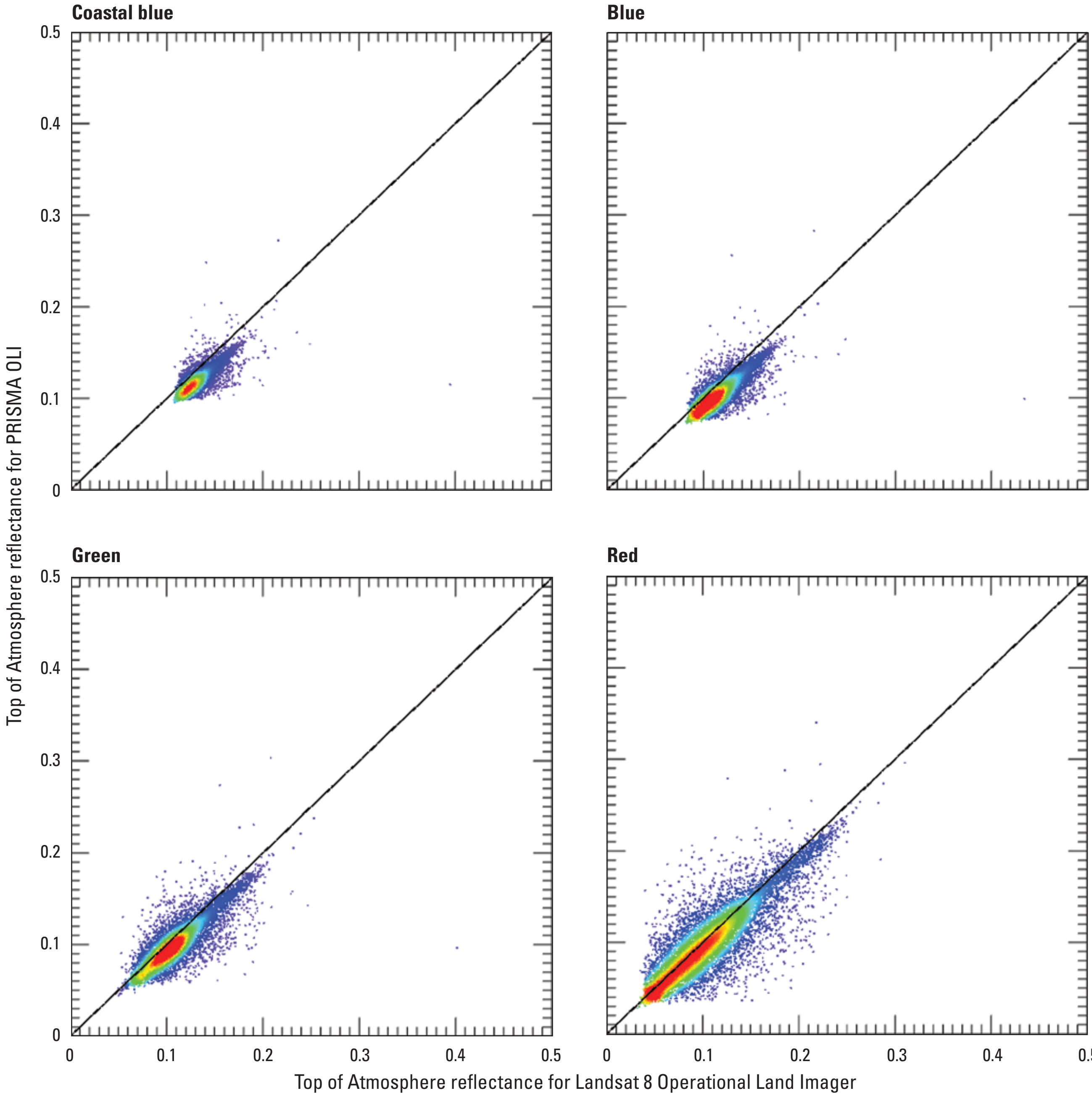

Figure 14. Top of Atmosphere reflectance comparison using image pair (La Roche-sur-Yon, France). [PRISMA OLI, PRecursore IperSpettrale della Missione Applicativa mimicking Operational Land Imager bands]

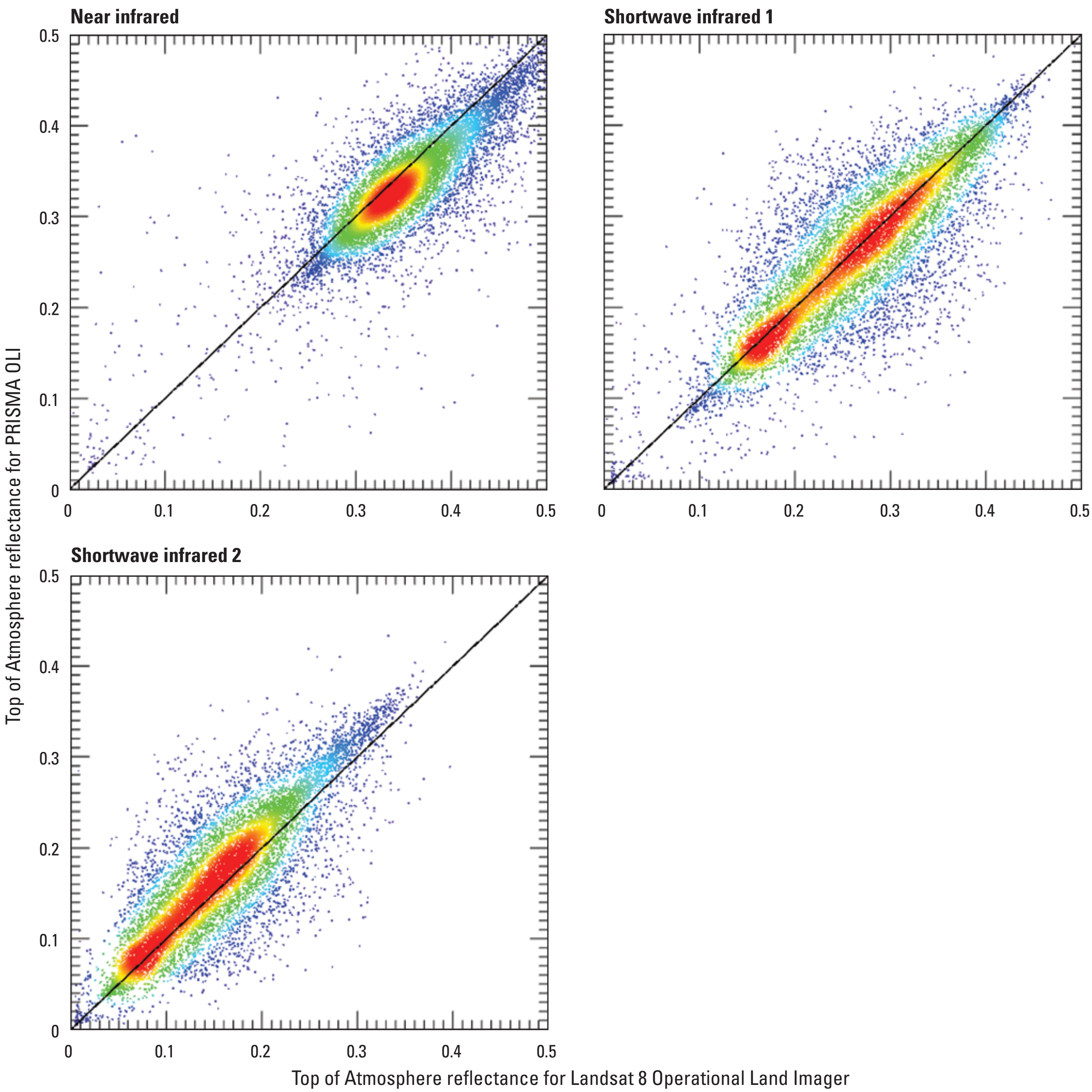

Figure 14. Top of Atmosphere reflectance comparison using image pair (La Roche-sur-Yon, France). [PRISMA OLI, PRecursore IperSpettrale della Missione Applicativa mimicking Operational Land Imager bands]—Continued

Spatial Performance

For this analysis, edge spread and line spread functions were calculated with resulting relative edge response, full width at half maximum, and modulation transfer function at Nyquist frequency analysis outputs, as listed in table 6. The PRISMA image used for spatial analysis is PRS_L1_STD_OFFL_20200412034634_20200412034638_0001.he5, and it is shown in figure 15.

The results for band 3 (green) are shown in figures 16 and 17. In figure 16, the raw transects, the middle transect, and the region of the curve that is used for alignment are shown. The lower plot in figure 16 is the aligned curve, and the edge spread function is shown. In the upper plot in figure 17, the edge spread function, relative edge response, line spread function, and full width at half maximum are shown. The lower plot in figure 17 is the modulation transfer function up to Nyquist frequency (0.5), and the frequency corresponding to the 50-percent modulation transfer function value is shown. The results for band 4 (red) are shown in figures 18 and 19, and the results for band 6 (first shortwave infrared band) are shown in figures 20 and 21.

Table 6. Spatial performance of the Italian Space Agency's PRecursore IperSpettrale della Missione Applicativa.

[RER, relative edge response; FWHM, full width at half maximum; MTF, modulation transfer function; SW, shortwave infrared]

Spatial analysis	RER	FWHM	MTF at Nyquist
Band 3—green	0.56	1.97 pixels	0.066
Band 4—red	0.60	1.95 pixels	0.054
Band 6—SW1	0.63	1.84 pixels	0.096

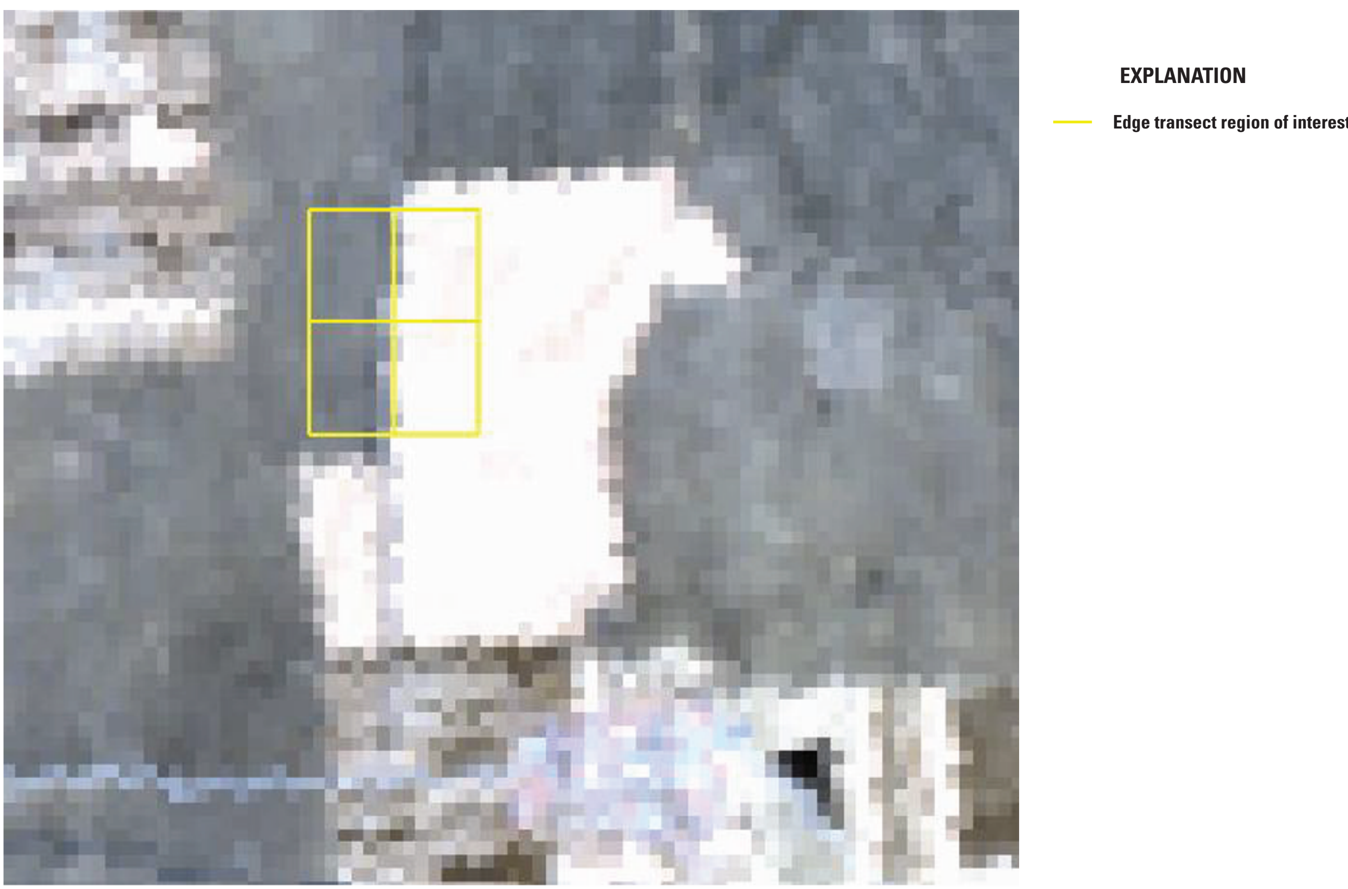

Figure 15. The Italian Space Agency's PRecursore IperSpettrale della Missione Applicativa region of interest for spatial analysis.

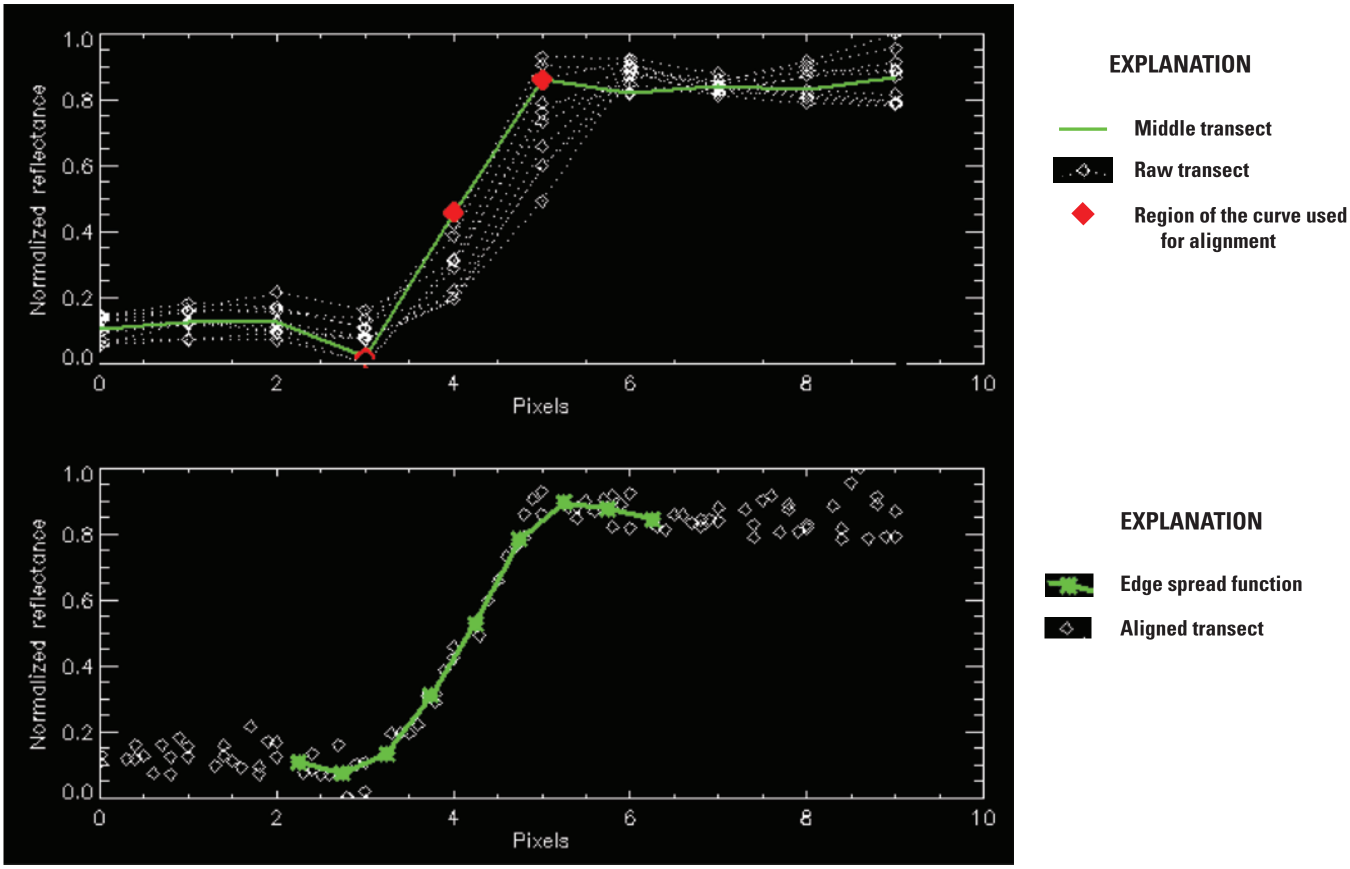

Figure 16. Band 3 (green) raw edge transects (upper) and aligned transects (lower).

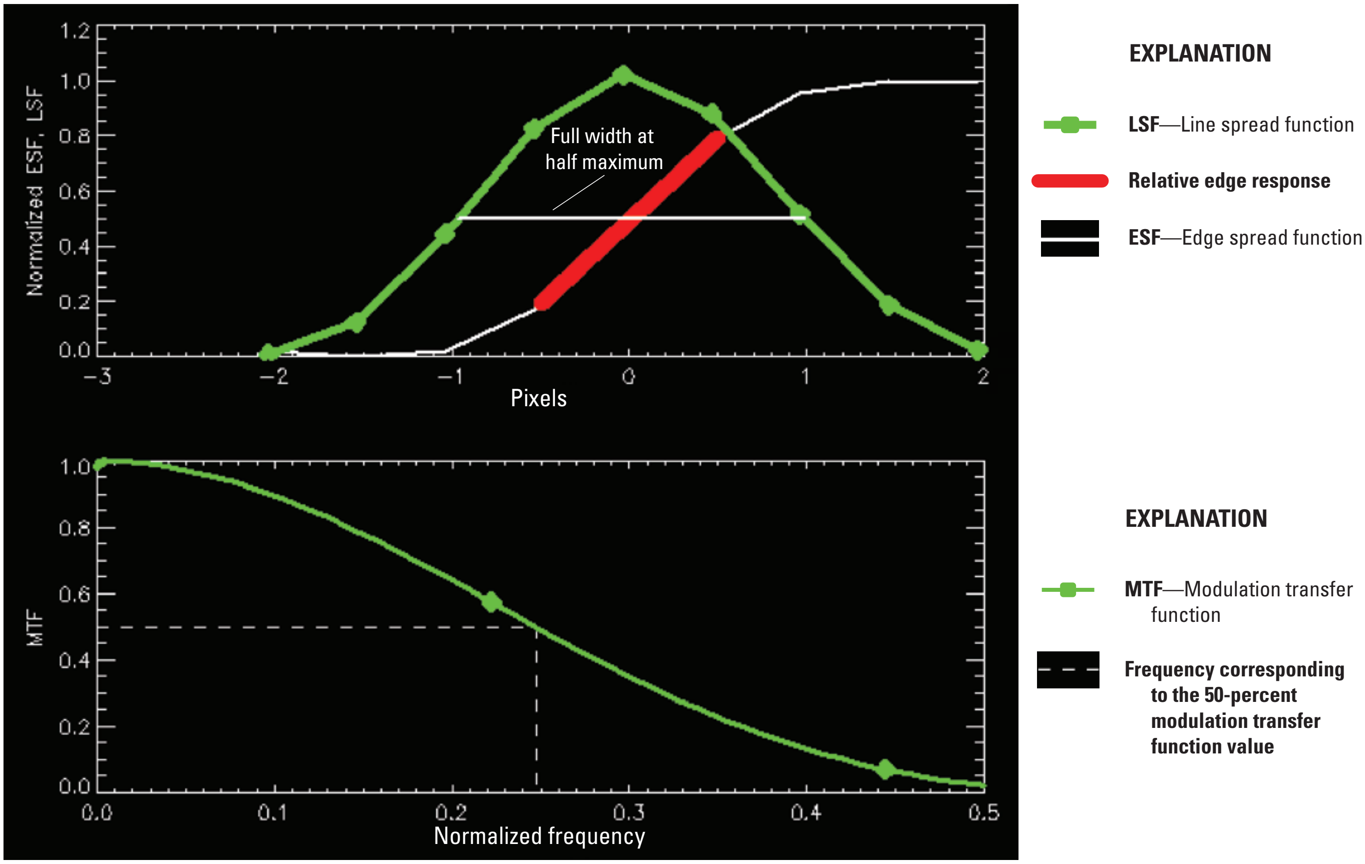

Figure 17. Band 3 (green) edge spread function and line spread function (upper) and modulation transfer function (lower).

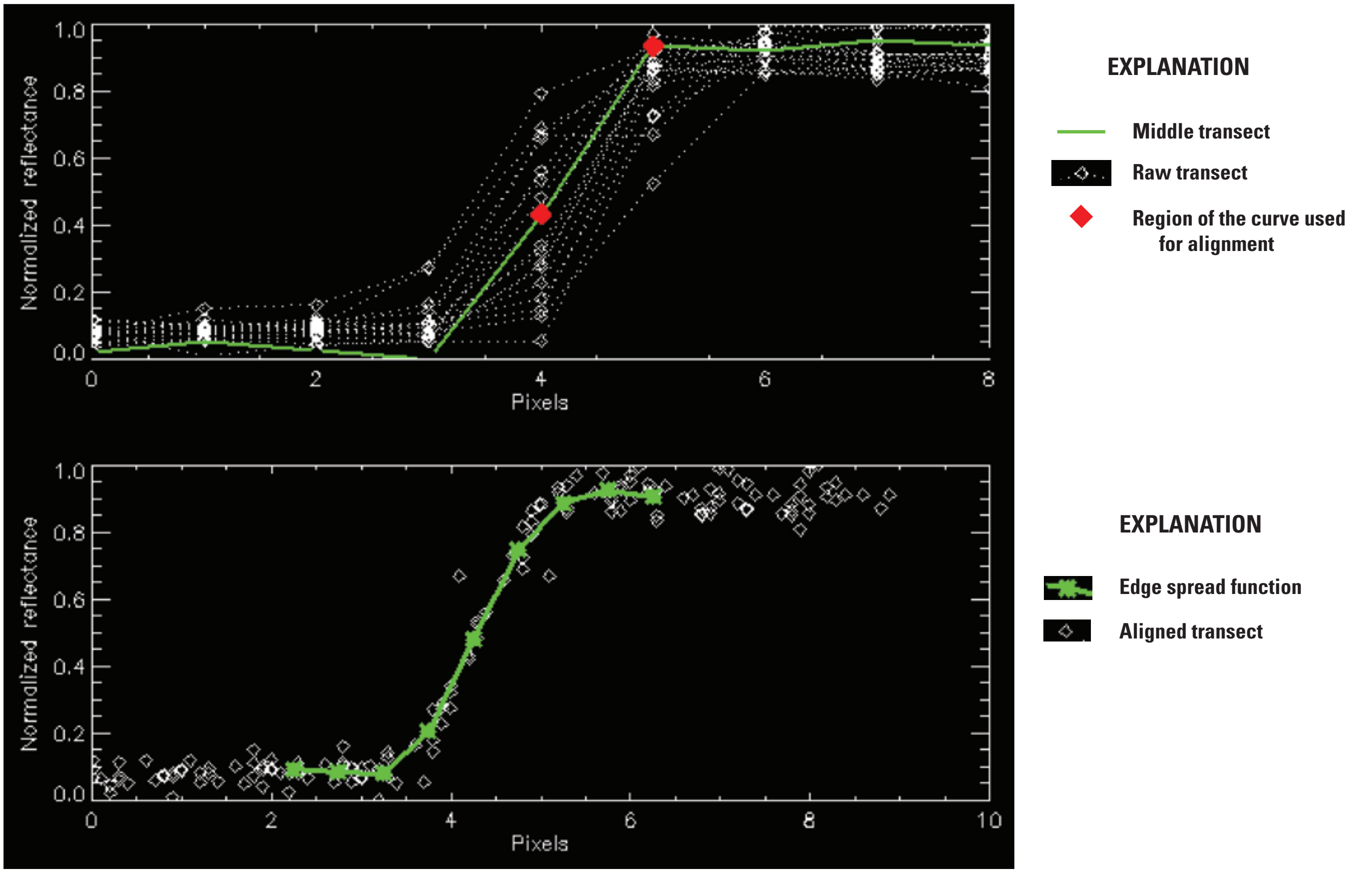

Figure 18. Band 4 (red) raw edge transects (upper) and aligned transects (lower).

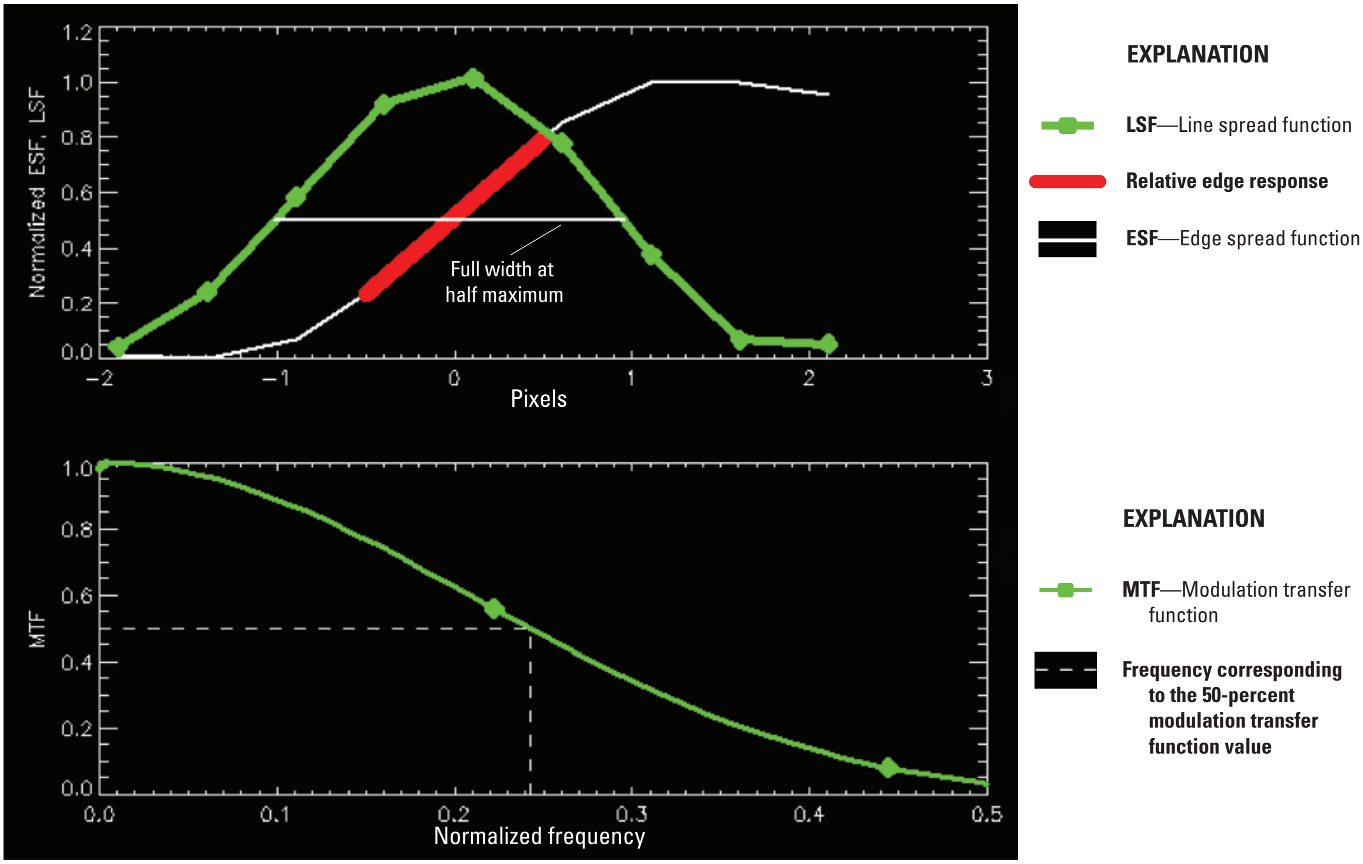

Figure 19. Band 4 (red) edge spread function and line spread function (upper) and modulation transfer function (lower).

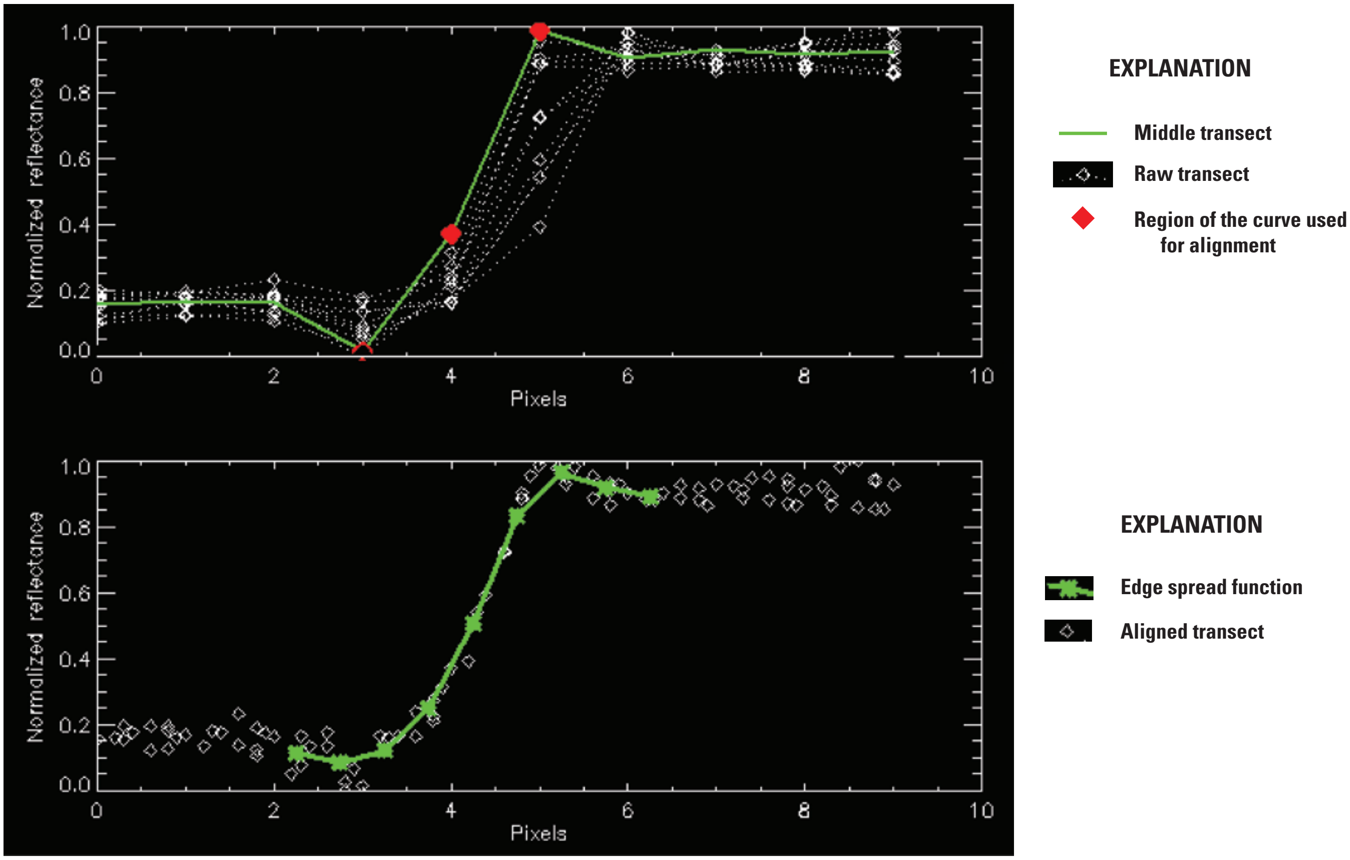

Figure 20. Band 6 (first shortwave infrared) raw edge transects (upper) and aligned transects (lower).

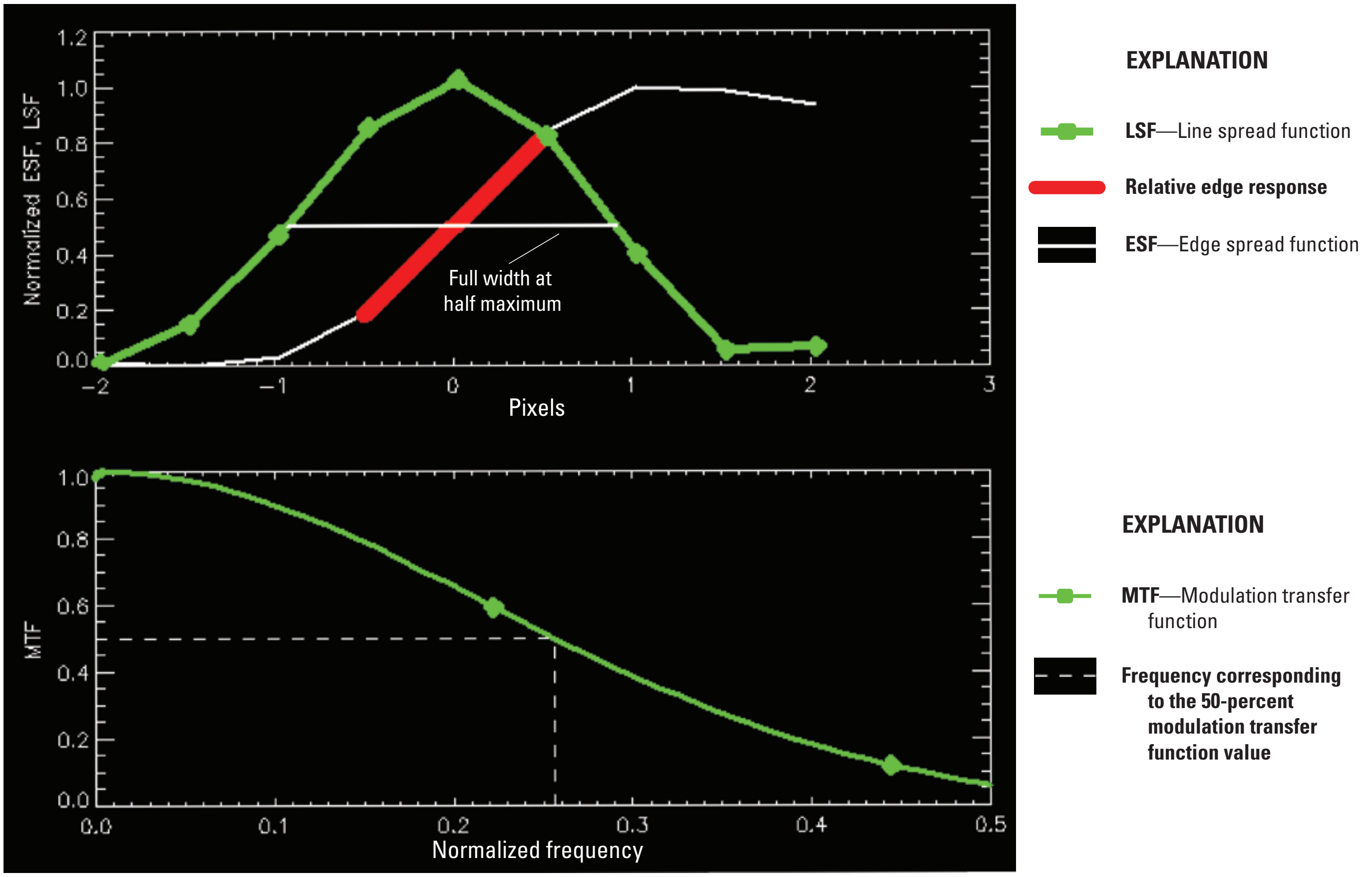

Figure 21. Band 6 (first shortwave infrared) edge spread function and line spread function (upper) and modulation transfer function (lower).

Summary and Conclusions

This report summarizes the sensor performance of the Italian Space Agency's PRecursore IperSpettrale della Missione Applicativa (PRISMA) based on the U.S. Geological Survey Earth Resources Observation and Science Cal/Val Center of Excellence (ECCOE) system characterization process. In summary, we have determined that the PRISMA sensor has a band-to-band geometric performance in the range of −0.046 to 0.040 pixel; an image-to-image geometric performance (relative to the Landsat 8 Operational Land Imager) in the range of −60.791 meters (m; −2.03 pixels) to 299.541 m (9.98 pixels); a radiometric performance in the range of −0.037 to −0.001 in offset and 1.026 to 1.274 in slope; and a spatial performance with a relative edge response in the range of 0.56 to 0.63, full width at half maximum in the range of 1.84 to 1.97 pixels, and a modulation transfer function at a Nyquist frequency in the range of 0.054 to 0.096.

Regarding fairly large geometric accuracy, the following explanation is provided to help the reader. The geometric accuracy required for PRISMA is a 200-m circular error at 90 percent (CE90) without ground control points (GCPs), a 15-m CE90 using GCPs is documented in the PRISMA mission overview (Agenzia Spaziale Italiana, 2021). The PRISMA images used for the current system characterization were georeferenced without using any GCPs; thus, the 200-m geometric accuracy requirement is applied. Beginning in 2022, a worldwide GCP database will be used in the PRISMA product processing chain, which will improve georeferencing accuracy to meet the 15-m CE90 requirement.

In conclusion, the team has completed an ECCOE standardized system characterization of the PRISMA sensing system. Although the team followed characterization procedures that are standardized across the many sensors and sensing systems under evaluation, these procedures are customized to fit the individual sensor as was done with PRISMA. The team has acquired the data, defined proper testing methodologies, carried out comparative tests against specific references, recorded measurements, completed data analyses, and quantified sensor performance accordingly. The team also endeavored to retain all data, measurements, and methods. This is key to ensure that all data and measurements are archived and accessible and that the performance results are reproducible.

The ECCOE project and associated Joint Agency Commercial Imagery Evaluation partners are always interested in reviewing sensor and remote sensing application assessments and would like to see and discuss information on similar data and product assessments and reviews. If you would like to discuss system characterization with the U.S. Geological Survey ECCOE and (or) the Joint Agency Commercial Imagery Evaluation team, please email us at eccoe@usgs.gov.

Selected References

Agenzia Spaziale Italiana, 2021, PRISMA: Agenzia Spaziale Italiana web page, accessed March 2021 at https://www.asi.it/en/earth-science/prisma/.

Ramaseri Chandra, S.N., Christopherson, J.B., and Casey, K.A., 2020, 2020 Joint Agency Commercial Imagery Evaluation—Remote sensing satellite compendium (ver. 1.1, October 2020): U.S. Geological Survey Circular 1468, 253 p. [Also available at https://doi.org/10.3133/cir1468.] [Supersedes USGS Circular 1455.]

U.S. Geological Survey, 2020a, EROS CalVal Center of Excellence (ECCOE): U.S. Geological Survey web page, accessed March 2021 at https://www.usgs.gov/calval.

U.S. Geological Survey, 2020b, EROS CalVal Center of Excellence (ECCOE)—JACIE: U.S. Geological Survey web page at https://www.usgs.gov/core-science-systems/eros/calval/jacie, accessed August 2021 at https://www.usgs.gov/core-science-systems/eros/calval/jacie?qt-science_support_page_related_con=3#qt-science_support_page_related_con.

U.S. Geological Survey, 2020c, Landsat missions—Glossary and acronyms: U.S. Geological Survey web page, accessed March 2021 at https://www.usgs.gov/core-science-systems/nli/landsat/glossary-and-acronyms.

For more information about this publication, contact:
Director, USGS Earth Resources Observation and Science Center
47914 252nd Street
Sioux Falls, SD 57198
605–594–6151

For additional information, visit: https://www.usgs.gov/centers/eros

Publishing support provided by the
Rolla Publishing Service Center

USGS

Kim and others—**System Characterization Report on PRecursore IperSpettrale della Missione Applicativa (PRISMA)**—OFR 2021–1030–K

ISSN 2331-1258 (online)
https://doi.org/10.3133/ofr20211030K